

Dynamics of HIV-infected CD4⁺ T cells: implications for cure strategies.

by
Zheng Wang

A dissertation submitted to Johns Hopkins University in conformity with the requirements
for the degree of Doctor of Philosophy

Baltimore, Maryland
Jun 2018

Abstract

Despite effective antiretroviral therapy (ART), HIV-1 persists in all infected individuals as proviral DNA integrated within long-lived resting memory CD4⁺ T cells. The population of infected CD4⁺ T cells carrying replication-competent proviruses is the major barrier to HIV-1 cure. Several lines of evidence have demonstrated that cellular proliferation of infected cells contributes to HIV-1 persistence. This proliferative process is complicated by the fact that most infected cells carry defective proviruses and cells harboring replication-competent HIV die quickly upon viral reactivation. To elucidate mechanisms that drive proliferation of HIV-1-infected CD4⁺ T cells, we followed proliferation of cells carrying replication-competent HIV-1 induced by antigen stimulation or cytokine treatment and demonstrated that latently infected cells carrying replication-competent HIV can proliferate in response to both stimuli. To study the dynamics of cells carrying replication-competent HIV-1, we sampled infectious virus from p24⁺ wells of the quantitative viral outgrowth assay at multiple time points spanning 2-3 years. Sequencing of replication-competent HIV-1 at multiple time points revealed that expanded cellular clones containing replication-competent HIV-1 is common. While some clones persist for 2-3 years, other clones wax and wane overtime. A similar pattern is observed with virus clones in the residual viremia. This observation with residual viremia supports our hypothesis that viruses in plasma are produced by activation of latently infected cells carrying replication-competent HIV-1 rather than ongoing cycles of virus replication. In addition, this supports our hypothesis that antigens drive proliferation of cells carrying replication-competent HIV-1 and activate some of the cells, leading to virus production. The observed patterns with proviruses in the latent reservoir and viruses in the residual viremia do not support a continuous proliferative process related to HIV-1 integration into cancer-associated genes.

These studies are also being extended to cells carrying defective proviruses. A previous study has demonstrated that defective HIV-1 proviruses can be transcribed, translated or even recognized by HIV-1 specific CD8⁺ T cells. We hypothesized that defective proviruses may have a proliferative advantage that allows the cells carrying defective proviruses to proliferate more than cells carrying intact proviruses. Given that intact proviruses only account for 2% of total proviruses in patients on long-term suppressive ART, infected cells carrying defective proviruses greatly outnumber the cells harboring intact proviruses *in vivo*.

We hypothesized that *in vitro*, cells carrying defective proviruses would proliferate upon T cell activation while cells harboring intact proviruses capable of viral gene expression, would die upon T cell activation due to viral cytopathic effects. Therefore, cells carrying either defective proviruses and or intact proviruses would show different proliferation dynamics upon TCR activation *in vitro*. To determine whether cells infected with intact or defective proviruses would proliferate to the same extent, we subjected single HIV-1 infected cells to 4 rounds of anti-CD3/CD28 stimulation in a microculture system and used a novel droplet digital PCR assay (intact proviral DNA assay; IPDA) to quantitate the number of intact and defective proviral DNA sequences in infected cells. We demonstrated that cells carrying defective proviruses were capable of enormous expansion with *in vitro* anti-CD3/CD28 stimulation, while cells harboring intact proviruses were rarely detected and showed little proliferative potential. Integration site analysis of clones expanded *in vitro* demonstrated that HIV-1 provirus integration into cancer-associated gene is not required for proliferation of HIV-1-infected cells. Additionally, we sequenced the cell clones that proliferated the most *in vitro* and found that proviruses in these clones were highly defective. These microculture experiments revealed a profound proliferation defect for cells carrying intact proviruses upon anti-CD3/CD28 stimulation.

To explore whether cells carrying intact and defective proviruses show similar dynamics *in vivo*, we examined longitudinal samples collected 2-8 years apart using the IPDA. We found that the half-life of infected was ~44 months, consistent with a previous measurements of the latent reservoir as measured with a quantitative viral outgrowth assay (QVOA), while cells carrying defective proviruses showed greater variability among patients. Collectively, my thesis has measured the dynamics of CD4+ T cells carrying different types of proviruses and has provided insight into mechanisms that may contribute to proliferation of HIV-infected cells *in vivo*.

Advisor: Dr. Robert Siliciano

Reader: Dr. Janet Siliciano

Preface

I would like to thank my mentor, Dr. Robert Siliciano, who has been so supportive throughout my doctorate training. I really appreciate the opportunities and resources Bob has given me to work in his lab and work on projects I am interested in. Bob has always been a role model to me. He sets a great example of doing rigorous science. I also want to thank Dr. Janet Siliciano, who has been such a good mentor in both lab and life. I am grateful for all the help and support I got from my lab members, especially from Dr. Ya-Chi Ho, Dr. Nina Hosmane, Dr. Christopher Pohlmeier, Dr. Gregory Laird and Jun Lai, who taught me the techniques and passed on their knowledge to me. I want to thank Dr. Andrea Cox and Dr. Joel Pomerantz. As members of my thesis committee, they have provided input that shaped my projects and invaluable career advice.

I have to thank my family, especially my parents, who encouraged me to pursue what I want to do and have been supportive of my decision to spend most of my time in a different country. I want to thank my friends from middle school, college and in the lab. Their support and all the good times we had together are invaluable to me. Lastly, I want to thank my husband Ming. It's very lucky of me to have him as a stabilizing force in my life.

Table of Contents

| | |
|--|------------|
| Abstract | ii |
| Preface | iv |
| Table of Contents | v |
| List of Tables and Figures | vii |
| | |
| Introduction | 1 |
| Chapter One: Dynamics of cellular clones carrying replication-competent HIV-1 | 10 |
| Introduction | |
| Materials and Methods | |
| Results | |
| - CD4+ T cells containing replication-competent virus can proliferate in response to T cell receptor (TCR) activation and cytokine treatment | |
| - Some expanded clones harboring replication-competent virus persist overtime while others wax and wane | |
| - Clonal populations of free plasma virus change overtime | |
| Discussion | |
| | |
| Chapter Two: Evaluating the role of HIV provirus in persistence of infected cells: implications for cure strategies | 33 |
| Introduction | |
| Materials and Methods | |
| Results | |
| - Analysis of HIV proviral sequences | |
| - Development and validation of intact proviral DNA assay (IPDA) | |

- HIV latent reservoir change measured by QVOA and IPDA
- Differential dynamics of cells carrying intact and defective proviruses

Discussion

| | |
|-------------------------|-----------|
| References | 59 |
| Curriculum Vitae | 66 |

List of Tables and Figures

| | |
|---|-----------|
| Table 1: Characteristics of HIV-1 infected study participants for Chapter 1 | 53 |
| Table 2: Characteristics of HIV-1 infected study participants for Chapter 2 | 54 |
| Table 3: Integration site analysis from microcultures | 56 |
| Table 4: Primers and probes for IPDA | 58 |
| Figure 1: Proliferation of infected cells in response to TCR stimulation and cytokines. | 20 |
| Figure 2: Expanded clones carrying replication-competent HIV-1 emerge and wane over time. | 23 |
| Figure 3: Neighbor-joining phylogenetic tree constructed with env sequences from the plasma and resting CD4+ T cells from subject S16. | 27 |
| Figure 4: Plasma virus clones wax and wane over a time scale of years. | 28 |
| Figure 5: Composite graph illustrating the appearance and longevity of clonal populations of free plasma virus and provirus from resting CD4+ T cells. | 30 |
| Figure 6: Standard DNA and Alu-PCR assays predominantly measure defective proviruses. | 41 |
| Figure 7: Use of full genome sequences to position amplicons for distinguishing intact and defective HIV-1 proviruses. | 43 |
| Figure 8: Intact proviral DNA assay (IPDA). | 45 |
| Figure 9: IPDA reproducibility. | 46 |
| Figure 10: Linearity of the IPDA. | 47 |
| Figure 11: IPDA reveals differential dynamics of intact and defective proviruses. | 50 |

Introduction

Despite prevention efforts, there are approximately 36.7 million people living with human immunodeficiency virus type 1 (HIV-1) infection worldwide. To date, only one person has been cured of an established HIV-1 infection. This has suggested that cure of HIV infection is possible. I will describe this case and other near cure cases and discuss why the latent reservoir in resting, memory CD4+ T cells is the major barrier to curing HIV-1 infection. I will also review HIV-1 latent reservoir dynamics as measured by current assays and present a novel assay that allows quantification of infected cells carrying different types of HIV-1 proviruses.

HIV-1 is a lentivirus that mainly replicates in activated CD4+ T lymphocytes and kills them quickly, usually within a day. In untreated infected individuals, infected CD4+ cells gradually decline over the course of several years. AIDS (acquired Immunodeficiency syndrome) is defined when the CD4+ T cells reach a threshold of 200 cells/ul in the blood and the infected individual is susceptible to opportunistic infections. AIDS is a condition in humans in which progressive destruction of CD4+ T cells allows life-threatening infections and cancers to thrive. Without lifelong antiretroviral therapy, most infected individuals will die from AIDS. The disease that we now call AIDS was first described in previously healthy homosexual men (1). Four patients had no preexisting immunodeficiency, but were anergic and lymphopenic, showing no lymphocyte proliferative responses to antigens. These patients contracted multiple viral infections and had prolonged fevers of unknown origin (1). Cytomegalovirus (CMV) was recovered from all four patients studied, but the persistence of fever and the occurrence of leukopenia, lymphopenia and opportunistic infection are not features of CMV infection in normal hosts. Therefore doctors concluded that the CMV and opportunistic infections might be a result of immunodeficiency observed in these patients (1).

To date, only a single person, the "Berlin patient", Timothy Brown, has been cured of an established HIV-1 infection. Mr. Brown was HIV-1 infected and doing well on antiretroviral therapy when he developed acute myeloid leukemia. To treat his leukemia, he received a bone marrow transplant from a carefully selected donor who was homozygous for a 32 base pair deletion in CCR5, a receptor that is critical for HIV-1 entry into CD4+ T cells. The Berlin patient has remained off antiretroviral therapy since the time of his initial transplant, now going on 10 years, and shows no sign of HIV-1 infection after the transplant (2). The Berlin patient is an important proof-of-principle case. Mr. Brown's immune system, including latently infected

resting CD4+ T cells were largely eliminated by the conditioning regimen that he received prior to his transplant and by graft vs. host disease after the transplant. Even if small numbers of infected cells remained and they produced virus, that virus could not reignite infection because Mr. Brown's new immune system was resistant to HIV-1 infection. However, this approach is not feasible for the 35 million infected individuals throughout the world since bone marrow transplant is a risky and expensive procedure and would most likely only be done on patients with certain malignancies. Efforts to reproduce this sterilizing cure in other patients have not resulted in additional cure. Two other patients, referred to as the "Boston patients", received transplants from donors with the wild-type CCR5 for malignancies to recapitulate the Berlin patient case. The Boston patients were different from the Berlin patient since their donor cells were fully susceptible to HIV-1 infection. These two patients remained on cART during the transplant period and for several years thereafter. When a variety of different assays to detect HIV-1 were negative, antiretroviral therapy was stopped because it was thought that these 2 patients were cured. Neither patient had detectable HIV-1 DNA in peripheral blood mononuclear cells (PBMCs) nor was infectious virus was recovered from co-cultures, which suggested elimination of infected cells in these patients. However, viral rebound was observed in the Boston patients 3 and 8 months after discontinuing cART. These cases demonstrate the presence of a stable latent reservoir in infected individuals and this latent reservoir persists for years with cART. It is essential to eliminate the latent reservoir to achieve a sterilizing cure.

Another case that provides insight into cure strategy is the "Mississippi Baby" (3). The child was born prematurely in a Mississippi clinic in 2010 to an HIV-1-infected mother who did not receive antiretroviral medication during pregnancy and was not diagnosed with HIV infection until the time of delivery. Because of the high risk of HIV-1 exposure, the infant was put on cART at 30 hours of age. Within several days of birth, the infant was diagnosed of HIV-1 infection. The baby was kept on cART until 18 months of age but was no longer receiving treatment afterwards. When medical staff saw the child again 5 months later, the child had undetectable HIV-1 level and showed no HIV-1 specific antibodies. The child continued to do well in the absence of cART and showed no sign of HIV-1 infection until recently. The child, now almost 4 years of age, was found to have detectable HIV-1 levels in the blood and decreased levels of CD4+ T cells. The case of the Mississippi baby child indicated that early antiretroviral treatment did not completely eliminate the latent reservoir, but it may alter the establishment and long-term persistence of HIV-1 infection.

Although combination antiretroviral therapy (cART) reduces viremia to undetectable levels, cART is not curative, and infected individuals must remain on therapy for life. Here I will review the barrier to achieving a cure by first discussing viral dynamics in infected individuals. I will then discuss potential cure strategies some of which are currently in various clinical trials. The main target of HIV-1 is activated CD4 T lymphocytes (4). The HIV-1 replication cycle starts with virus binding to cell surface receptor CD4 and chemokine co-receptors CXCR4 or CCR5; cell entry, reverse transcription of the viral RNA to double stranded cDNA; uncoating of the viral capsid, nuclear import of viral cDNA within the pre-integration complex; and DNA integration (4). Entry of virus requires interaction with CD4 and the chemokine coreceptors, CCR5 or CXCR4 (5, 6). However, viral entry into target cells does not guarantee viral replication due to the existence of host restriction factors that can target HIV-1. These host restriction factors include Apolipoprotein B mRNA-editing enzyme 3G (APOBEC3G) and SAMHD1 (7). Following transmission, there is rapid virus replication in activated CD4+ T cells and a rapid increase in the level of plasma virus (4). This increase is exponential. This exponential virus replication generates immune responses that reduce viremia to a quasi-stable set point in about one month. This exponential virus replication drives CD4+ T cell depletion, leading eventually to fatal immunodeficiency in an untreated patient. However, combination antiretroviral therapy causes rapid, exponential biphasic decay in plasma virus (viremia) to below the limit of clinical detection, 50 copies of viral RNA/ ml plasma. Although ART cannot target the latent reservoir, clinical studies have demonstrated that an optimal ART regimen can inhibit ongoing cycles of HIV-1 replication. The first antiretroviral drug approved by FDA is zidovudine (3'- azido-3'-deoxythymidine (AZT)), a thymidine analogue that inhibits reverse transcription of HIV-1 (8-10). However, AZT monotherapy selects for drug resistance, which in turn spurred the development of other classes of drugs, including: other nucleoside analogue reverse transcriptase inhibitors (NRTIs), protease inhibitors (PIs), non-nucleoside reverse transcriptase inhibitors (NNRTIs), fusion inhibitors, entry inhibitors and integrase inhibitors. Combination antiretroviral therapy (cART) became a standard treatment regimen that reduced HIV-1 infection to a manageable, chronic disease (11, 12). The antiretroviral drugs block new cells from becoming infected but do not prevent virus release from infected cells that already have an integrated provirus. Therefore, the biphasic exponential decay in viremia after initiation of cART reflects the rapid turnover of two infected cell populations that have very short half-lives and produce most of the plasma virus. Unfortunately, this decay does not continue but rather plateaus at

a new steady state of ~ 1 copy virus /ml plasma (13). This small amount of residual viremia is not due to continuous, ongoing cycles of virus replication because if you intensify a 3-drug antiretroviral regimen by adding a fourth, new drug, residual viremia does not go down (14-19). Rather, residual viremia reflects viruses that are being released by a third population of infected cells that were infected prior to the start of antiretroviral therapy and have an extremely long half-life. This population of infected cells are latently infected, resting memory CD4+ T cells and they arise as a consequence of the normal biology of CD4+ T cells. Upon encountering their specific cognate antigen, resting CD4+ T cells become activated and proliferate, generating many activated effector cells with the same antigen specificity. At the conclusion of the immune response, most of these activated, effector cells die, but some survive and return back to a resting memory state as long-lived memory CD4+ T cells. Memory cells allow for future responses to the same antigen. HIV-1 replicates mainly in activated CD4+ T cells, and these productively infected cells die quickly, usually within one day. However, if activated cells are infected with HIV-1 during the transition back to a resting memory state, then this results in a stably integrated but transcriptionally silent form of the viral genome in a long-lived memory CD4+ T cell, allowing viral persistence through mechanisms that maintain lifelong immunologic memory. In resting memory CD4+ T cells, HIV-1 gene expression is turned off as host transcription factors necessary for viral transcription are sequestered in the cytosol under resting conditions (20). Our lab many years ago developed assays to detect the presence and persistence of latently infected cells in patients virally suppressed on cART (21-26). Latently infected resting CD4+ T cells are present in all individuals infected with HIV-1. The presence of this population of latently infected cells was demonstrated by a quantitative viral outgrowth assay (QVOA). This population of infected cells is present at a very low frequency in patients; $\sim 1/10^6$ resting CD4+ T cells are latently infected with replication competent virus. However, longitudinal analysis in virally suppressed patients demonstrated that this infected cell population has an extremely long half-life of 44 months (27). Our analysis further showed that it would take ~ 70 years for a population of one million of these infected cells to turn over thereby guaranteeing that patients need to be on antiretroviral therapy for life. Therefore, HIV-1 infection is not curable due to the persistence of a small number of latently infected memory CD4+ T cells harboring replication-competent proviruses (23-25).

Different curative strategies targeting the latent reservoir have been proposed. The “sterilizing cure” approach involves purging the body of all latent proviruses so no virus would restart the infection if cART

were stopped. The “functional cure” approach would instead equip the immune system with the ability to control the virus without antiretroviral therapy (28, 29). The Berlin patient is a proof of principle case for the “sterilizing cure” approach but this approach could not be applied to most infected individuals. One potential approach to reduce the latent reservoir is known as “shock and kill” (30, 31). This strategy aims at inducing proviral expression to enable clearance of virally infected cells (32). In order to induce viral expression, T cell activation may be necessary. Early attempts to reactivate virus production via global T cell activation led to unexpected high levels of immune activation and were toxic to patients (33). Therefore, newer approaches have involved reversing latency without inducing T cell activation (33). The “shock-and-kill” strategy for HIV eradication envisions reversing latency by inducing viral gene expression so that infected cells die from viral cytopathic effects or immune clearance. A number of mechanistically distinct latency-reversing agents (LRAs) have been identified using *in vitro* models of latency. These include histone deacetylase (HDAC) inhibitors, thought to function by modifying the epigenetic environment around the site of provirus integration (34, 35); disulfiram, which involves nuclear factor kappa-light-chain-enhancer of activated B cells (NF- κ B) (32, 36, 37); the bromodomain-containing protein 4 (BRD4) inhibitor JQ1, which elicits transcription through positive transcription elongation factor (P-TEFb) (38-41); and protein kinase C (PKC) agonists such as bryostatin-1 and prostratin, which have a major role in signaling pathway downstream of T cell receptor engagement (42-45). Studies have shown that LRAs do not significantly cause proviral expression in patient cells (46). Clinical trials in patients on ART with disulfiram and HDAC inhibitors such as vorinostat, romidepsin and panobinostat showed inconsistent results (35, 36, 47-49). Most importantly, no LRA has been demonstrated to reduce the size of the latent reservoir (35, 36, 47-49). In addition, most candidate LRAs did not significantly increase viral gene expression. The only LRAs that work as single agents are protein kinase C agonists (PKCs) like bryostatin-1, which is consistent with the role of PKC in signaling pathways downstream of T cell receptor engagement and co-stimulation (46).

Other model systems of HIV-1 latency have been developed to test new intervention strategies, but none of these primary cell models fully recapitulates the complexities of the latent reservoir *in vivo*. Some of the most commonly used models include cell line models derived from immortalized T cell clones, primary cell models derived from HIV-1-negative donor CD4+ T cells, humanized mouse models generated by engraftment of mice with human tissues, and non-human primate models (50). Animal models are ideal for

study of HIV-1 latency in the setting of cART treatment. Simian immunodeficiency virus (SIV) and recombinant viral strains such as SHIV are the most commonly used strains in non-human macaque models of infection as the pathogenesis and the establishment of a latent reservoir are similar to HIV-1 pathogenesis in humans. Recently, several studies in non-human primate studies have demonstrated that a combination of toll-like-receptor 7 (TLR7) agonist and broadly neutralizing antibodies could effectively delay viral rebound after the ART is stopped (51). PGT121 is a broadly neutralizing antibody that targets the V3 glycan site on the envelope and GS-9620 is a TLR7 agonist that stimulates TLRs on immune cells of the innate immune system. The most recent study included 11 rhesus macaques on cART infected with SHIV. After 2 years on cART, they received infusions of PGT121 and oral doses of GS-9620. Antiretroviral therapy was then discontinued 4 months after the last doses of PGT121 and GS-9620. Of the 11 monkeys that received this combination of PGT121 and GS-9620, 6 experienced viral rebound and 5 continued to maintain undetectable viral load for at least 168 days after stopping cART. Even after viral rebound, monkeys that received the combination treatment had a lower viral load set point in lymph nodes, suggesting a decrease in the size of the latent reservoir (52).

So far, no single LRA or LRA combination has induced a substantial amount of viral reactivation, as measured by viral RNA production. The major caveat with this “shock and kill” strategy is that successful induction of viral expression does not guarantee that infected cells will die (53). Clearance of infected cells will require a second step involving a potent and efficient immune response. Other observations further complicate the “shock and kill” strategy include: insufficient number and function of HIV-specific CD8+ T cells and natural kill (NK) cells, disperse and scarce HIV antigen expression in latently infected cells, and the existence of viral populations evolved to escape CD8+ T cells killing (54-56) and escape from neutralizing antibodies. A previous study demonstrated that latency reversal does not lead to reservoir reduction (57). Pre-stimulation of these HIV-specific CD8+ T cells with HIV peptides is required to increase the number and enhance the killing ability of these CD8+ T cells (58-60). Additionally, studies looking into the role of other effector cells, such as NK cells also suggested that “priming” of the effector cells is required to restore the function of the effector cells (61). Together, these results suggest that some level of vaccination may be necessary to activate the immune responses following viral reactivation for infected cell clearance.

In order to come up with an effective cure strategy, we need to obtain a better understanding of the latent reservoir. Previous studies looking into residual viremia in patients on cART have demonstrated that trace level of free virus in the plasma could not be reduced by treatment intensification or adding additional drugs. By sequencing the viruses in plasma, it has been shown that these viruses are continually released for years without sequence evolution in patients on cART (62, 63). These early studies indicate that the residual viremia arises from the daily activation of a small number of latently infected cells rather than from new cycles of replication. Interestingly, in most infected individuals, the residual viremia is dominated by a population of viruses with identical sequences (63). The clonal nature of the residual viremia suggests that it is produced by limited number of cells carrying identical HIV proviruses, which is likely to be a result of cellular proliferation. These results provided the first evidence for proliferation of latently infected cells, which copies the viral genome without error into progeny cells and contributes to HIV persistence. Several recent studies used HIV integration site analysis to provide definitive evidence for cellular proliferation of HIV-infected cells in individuals on cART (64, 65). These studies demonstrated that a large fraction of the infected cells have undergone clonal expansion based on the presence of identical HIV integration sites in different infected peripheral blood lymphocytes collected at different time points (64, 65). Interestingly, these studies showed that a significant amount of the expanded clones have proviruses integrated into genes related to cell growth and suggested that HIV integration into cancer-associated genes may promote proliferation of the infected cells (64, 65). One caveat with the integration site analysis is that the method captures only a small part of the HIV proviral genome. Therefore it is likely that many of the expanded cellular clones captured by this method carry defective proviruses. Other studies used the QVOA to recover independent infectious viruses in infected individuals and revealed that a large fraction of the latent reservoir is comprised of infected cells that have undergone clonal expansion (66-69). To study the mechanisms responsible for clonal expansion of cells containing replication-competent proviruses, we tested several conditions that have been proposed to induce clonal expansion of HIV-infected CD4+ T cells, including antigen stimulation and cytokine-driven homeostatic proliferation (69, 70). To confirm the importance of antigen-driven proliferation and homeostatic proliferation in HIV persistence, we also examined the *in vivo* dynamics of clonal populations of infected cells carrying intact proviruses and characterized the mechanisms that could induce *in vivo* proliferation of infected cells harboring replication-competent HIV.

The QVOA demonstrated the presence of HIV latent reservoir in all HIV infected individuals and longitudinal analysis demonstrated that the latent reservoir in resting memory CD4+ T cells undergoes slow decay in individuals on cART (27, 71). As discussed above, proliferation of infected cells carrying replication-competent HIV is common (66, 68, 69). Therefore, the slow decay of the latent reservoir reflects a significant amount of proliferation of infected cells balanced by infected cell death. Studies that look into the dynamics of the latent reservoir provide insight into strategies that could dramatically reduce the size of the latent reservoir. Mathematical modeling suggested that even a 20% reduction in proliferation rate could effectively decrease the half-life of the latent reservoir. Therefore we should consider potential cure strategies that block proliferation of latently infected cells or speed up the decay of the latently infected cells.

The QVOA allows quantification of replication-competent provirus, but it has recently been shown to underestimate the size of the latent reservoir because one single round of T cell activation does not efficiently induce all replication-competent proviruses (66). The standard QVOA can thus be considered a definitive minimal estimate for the size of the latent reservoir, capturing only a fraction of the latent reservoir with a single round of stimulation and outgrowth. To better understand the proviral landscape in infected individuals, several methods have been developed to capture the sequence of individual provirus to distinguish defective proviruses from those intact ones that are potentially capable of replication. The importance of such sequencing-based approaches is underscored by the surprising results of two recent studies that used a novel single genome amplification method to define the proviral landscape and examined the nature of defects present in persistent HIV proviruses (72, 73). Using the single proviral-genome sequencing method, we interrogated the sequences of the proviruses present in the QVOA culture wells that were negative for viral outgrowth. The vast majority of the proviruses were defective, harboring either large internal deletions and/or APOBEC3G-mediated hypermutation (72). Additionally, a follow-up study examined proviral genomes from HIV-infected individuals in resting CD4+ T cells. In all individuals studied, only a fraction of the proviruses are intact. Many of the proviral genomes in these individuals are hypermutated and deleted. Importantly, the median frequency of cells carrying intact proviruses is more than 60-fold higher than what is detected by the standard QVOA (73).

A successful cure strategy would result in a drastic decrease in the size of the latent reservoir. Considering the low frequency of latently infected cell in infected individuals, an accurate and efficient

method is required for development and assessment of cure strategies. As discussed above, the QVOA gives us an absolute quantification of the minimal number of latently infected cells that can be induced to produce infectious virus with a single round of T cell activation. Multiple PCR-based methods have been developed to amplify sub-genomic regions and are used widely to measure the size of the reservoir (74, 75). The major caveat of these PCR-based methods is that they do not distinguish intact proviruses from defective proviruses, which are considered clinically irrelevant. Therefore PCR-based assays could lead to an overestimation in the size of the latent reservoir given that defective proviruses greatly outnumber intact proviruses in chronically treated individuals. In this thesis, I describe a novel digital droplet PCR based assay developed in our laboratory. The assay allows differential quantification of intact and defective proviruses and is used to measure the decay of different populations of proviruses. Using this intact proviral DNA assay (IPDA), I demonstrated that in most infected individuals, cells carrying intact proviruses undergo slow decay with a half-life close to that measured by the QVOA, while cells harboring defective proviruses showed greater variability that reflects proliferation or decline of these infected cells. I also examined the proliferative potential of cells carrying different types of proviruses using a microculture system. The results for *in vitro* proliferation of infected cells are consistent with our findings *in vivo* and provide insight into potential cure strategies for elimination of the latent reservoir.

The Berlin patient case has renewed optimism that curing HIV-1 is possible and has inspired new cure approaches. In this thesis, I provide a detailed analysis of dynamics of persistent proviruses both *in vivo* and *in vitro*. I believe knowledge of latent reservoir dynamics will further our understanding of the virus and the immune mechanisms associated with viral persistence.

Chapter One: Dynamics of cellular clones carrying replication-competent HIV-1

Introduction

The latent reservoir for HIV-1 in resting memory CD4⁺ T cells persists even in patients on optimal antiretroviral therapy (ART) and is the major barrier to cure (23, 25, 76). The reservoir is established early in infection (77, 78), and is extremely stable, with an estimated half-life of 44 months (6-8), making cure with ART alone unlikely. One strategy to eliminate the latent reservoir is termed shock-and-kill (9, 10). It depends on inducing proviral expression in latently infected cells to allow their elimination by immune mechanisms or viral cytopathic effects.

Previous studies suggested that the proliferation of infected cells might contribute to HIV-1 persistence (11-19). At least three mechanisms may explain the proliferation of infected cells: antigen-driven T cell proliferation (16), homeostatic proliferation (13), and proliferation driven by effects related to the site of HIV-1 integration (14, 15). Proliferation of infected cells driven by antigen or cytokines is unexpected because these stimuli also induce viral gene expression in latently infected cells (20, 21), which exposes the cells to viral cytopathic effects and immune clearance. *In vivo*, most productively infected cells have a short half-life (22, 23). Interestingly, it has been shown in a model system that latently infected CD4⁺ T cells can proliferate in response to cytokines such as IL-2 and IL-7 without viral reactivation (79).

Early evidence for the *in vivo* proliferation of HIV-1-infected cells came from detailed phylogenetic studies showing the presence in plasma of viruses with identical sequences termed 'predominant plasma clones' (PPCs) in some infected individuals on prolonged ART (11, 12). In treated patients who have suppression of viremia to below the limit of detection of clinical assays, this residual viremia can be detected with very sensitive assays (25-28). The residual viremia consists of archival viral sequences that are sensitive to the current drug regimen and that do not show evolution over time (12, 29-32). Numerous studies have shown that levels of residual viremia cannot be reduced by treatment intensification (33-35). All of these results suggest that residual viremia results from the daily activation of a small number of latently infected cells rather than ongoing cycles of replication. The clonal nature of residual viremia suggested that it is produced by limited subset of infected cells carrying identical HIV-1 sequences, likely arising as a result of cellular proliferation (11, 12).

Further support for the role of T cell proliferation in HIV-1 reservoir dynamics came from a landmark study that defined the distribution of latent HIV-1 among the central memory (T_{CM}), transitional memory (T_{TM}), and effector memory (T_{EM}) $CD4^+$ T cell subsets and the role of cytokine-driven homeostatic proliferation in reservoir stability (13).

More recent studies used HIV-1 integration site analysis to provide direct and definitive evidence for clonal expansion in infected cells in individuals on long-term ART (14, 15, 36). A large fraction of the infected cells appear to have undergone clonal expansion based on the presence of identical HIV-1 integration sites in different infected peripheral blood lymphocytes (14, 15, 36). One study described identical viral sequences integrated at exactly the same position in the human genome in multiple cells, consistent with infected cell proliferation (15). Two studies suggested that HIV-1 integration into genes associated with cell growth and survival might drive proliferation of infected cells (14, 15).

While clonal expansion of infected $CD4^+$ T cells is prevalent in infected individuals, most HIV-1 proviruses are defective (37, 38). Since integration site analysis captures only a small part of the HIV-1 genome, it is likely that many of the expanded cellular clones detected by this method harbor defective proviruses (36). However, a highly expanded clonal population of $CD4^+$ T cells harboring a replication-competent provirus was recently characterized in an infected individual with metastatic squamous cell carcinoma, suggesting that cells carrying replication-competent proviruses can expand and persist (16). In addition, three recent studies demonstrated that clonal $CD4^+$ T cell populations carrying replication-competent viruses are common in infected individuals, accounting for over 50% of the latently infected cells examined (17-19). Therefore it is crucial to evaluate how cells containing replication-competent provirus proliferate. This information may help us to understand the forces that shape and preserve the latent reservoir.

To address these issues, we asked whether infected $CD4^+$ T cells harboring replication-competent provirus could proliferate in response to TCR stimulation or cytokines that are known to drive homeostatic proliferation and if so, whether this proliferation can occur without viral reactivation. In addition, we examined the *in vivo* dynamics of clonal populations of infected cells carry replication-competent HIV-1 to determine whether and how expanded clones harboring replication-competent provirus persist over time.

Materials and Methods

Study subjects

Participants were HIV-1-infected individuals who had suppression of viremia to less than 20 copies HIV-1 RNA/ml on ART for more than 6 months. The Johns Hopkins Institutional Review Board approved this study, and written informed consent was obtained from all subjects.

Resting CD4⁺ T cell isolation and plasma sample processing

180 mL of blood was collected at each study visit using an acid-citrate-dextrose anticoagulant and processed as previously described (41). Briefly, plasma and cells were separated using a Ficoll density gradient. The plasma layer was quickly removed, centrifuged to remove any contaminating cells, and immediately frozen and stored at -80°C until further use. The buffy coat layer was subsequently removed, and resting CD4⁺ T cells were purified from total peripheral blood mononuclear cells (PBMC) via magnetic bead depletion as previously described (42).

Cell culture conditions

Approximately 10×10^6 cells were cultured untreated, or with anti-CD3/CD28 Dynabeads (25 μ l/million cells, Thermo Fisher Scientific) + IL-2 (30 U/ml) or with IL-7 (10 ng/ml, BioLegend) + IL-2 (30 U/ml) in RPMI plus 10% FBS for 7 days in the presence of tenofovir disoproxil fumarate (10 μ M) and emtricitabine (10 μ M).

TCR sequencing

Cell proliferating in response to anti-CD3/CD28 or IL-7 were sorted using Sony SH800 cell sorter based on CFSE dilution (see below). DNA was extracted from aliquots of resting CD4⁺ T cells and sorted cell populations (QIAGEN). Adaptive Biotechnologies performed TCR sequencing on extracted DNA.

CFSE dilution and activation marker staining

Total resting CD4⁺ T cells were stained with 5 μ M CFSE (Life Technologies) before stimulation with anti-CD3/CD28 or IL-7 as described above. The dilution of CFSE was analyzed 1 week later by flow cytometry on a

FACSCanto II cytometer (BD Biosciences). Unstimulated resting CD4⁺ T cells cultured for the same time period of time served as a negative control. Expression of activation markers was analyzed 1 week after initial stimulation. An aliquot of cells from each culture was stained with anti-CD25 (PerCP5.5), anti-CD69 (APC), and anti-HLA-DR (Pacific Blue) antibodies (BioLegend) at 4 °C for 15 min and analyzed by flow cytometry on the FACSCanto II cytometer.

Quantitative Viral Outgrowth Assay (QVOA)

The QVOA was performed on cultured, unsorted resting CD4⁺ T cells and on sorted cells that had proliferated in response to anti-CD3/CD28 or IL-7. The cells were plated at limiting dilution for viral outgrowth (200,000 cells in 2 ml media per well) (37). Cells were activated with 0.5 µg/ml PHA and γ-irradiated allogeneic PBMCs from healthy donors (1). On day 2, media with PHA was removed and replaced with fresh media, and 10⁶ MOLT-4/CCR5⁺ cells were added to each well to allow expansion of virus released from cells in which latency had been reversed (42). MOLT-4/CCR5⁺ cells were obtained from the National Institutes of Health AIDS Reagent Program. CCR5 receptor expression on MOLT-4/CCR5⁺ cells was routinely tested by flow cytometry. On day 5, 0.75 ml media was removed and cells in each well were resuspended. Media was changed on days 5 and 9. A p24 ELISA (PerkinElmer) was performed on the supernatant on day 14 of the culture. Limiting dilution maximum likelihood statistics were used to calculate the frequency of latently infected cells (<http://silicianolab.johnshopkins.edu/>) (80).

RNA isolation, cDNA synthesis, and amplification of the *env* gene from proviruses in resting CD4⁺ T cells

Viral RNA isolation was performed on 200 µl of the supernatant from each p24⁺ well using a ZR-96 Viral RNA kit (Zymo Research Corporation). Isolated RNA was treated with DNase (Thermo Fisher Scientific) and used for cDNA synthesis using the qScript cDNA Supermix kit (Quanta Biosciences). We then ran a nested PCR on cDNA from each p24⁺ well targeting the V3-V4 region of *env*. The nested PCR was performed using 500 ng cDNA and primers ES7 (5'-CTGTTAAATGGCAGTCTAGC-3') and ES8 (5'-CACTTCTCCAATTGTCCCTCA-3') for the outer reaction. The outer PCR products were then diluted 1:50, and 5 µl of this diluted outer PCR product was used for the inner PCR reaction with primers Nesty8 (5'-CATACATTGCTTTTCCTACT-3') and DLoop (5'-GTCTAGCAGAAGAAGAGG-3'). Primers were obtained from Integrated DNA Technologies. Detailed

amplification conditions were: 94°C for 30 s, then 94°C for 30 s, 55°C for 30 s and 68°C for 2 m for 39 cycles; then 68°C for 5 m. PCR products were visualized on 1% agarose gels, and bands were extracted using the QIAquick Gel Extraction kit (QIAGEN). Extracted DNA was analyzed directly by Sanger sequencing at Genewiz, Inc.

Amplification and sequencing of the *env* gene from plasma virus

Free virus in the plasma of treated patients was analyzed as previously described (12). Briefly, 6 mL aliquots of plasma were thawed and ultracentrifuged at $170,000 \times g$ for 30 minutes at 4°C. Pelleted virus was resuspended in 400 μ L of phosphate buffered saline (PBS) (Invitrogen) and lysed, and the RNA extracted via a silica bead-based RNA isolation protocol, implemented on an EZ1 Biorobot (Qiagen). The RNA was eluted in 60 μ L of elution buffer and subsequently treated with amplification grade DNase I (Invitrogen), according to the manufacturer's instructions. To amplify the C2-V4 region of the *env* gene from RNA isolated from free plasma virus, the RNA was subjected to a one-step reverse transcriptase (RT)-PCR using a Superscript III reverse transcriptase/Platinum Taq high fidelity DNA polymerase one-step RT-PCR kit (Invitrogen) followed by a nested PCR, using Platinum Taq high fidelity DNA polymerase, and 2.5 μ L of the outer reaction as template. Control reactions were carried out for all experimental amplifications, including a no RT control to rule out DNA contamination and a no template control. Primers for the outer and nested reactions were as follows: (outer forward) 5' - CTGTTAAATGGCAGTCTAGC - 3', (outer reverse) 5' - CACTTC TCCAATTGTCCCTCA - 3', (nested forward) 5' - ACAATGCTAAAACCATAATAGT - 3', (nested reverse) 5' - CATAATTGCTTTTCCTACT - 3'. PCR conditions for the one-step RT-PCR were as follows: reverse transcription at 50°C for 30 minutes, denaturation at 94°C for 3 minutes, followed by 40 cycles of 94°C for 30 seconds, 55°C for 30 seconds, and 68°C for 1 minute. The PCR conditions for the nested reaction were as follows: denaturation at 94°C for 3 minutes, followed by 40 cycles of 94°C for 30 seconds, 55°C for 30 seconds, and 68°C for 1 minute. Products of the nested reaction were separated on 1% agarose gels. Bands of appropriate size were excised, and the corresponding amplicons were eluted using QIAquick gel extraction kits (Qiagen). Isolated amplicons were subsequently cloned using a PCR2.1 TOPO cloning vector (Invitrogen), and at least 6 clones were sequenced from each PCR using an ABI Prism 3700 DNA analyzer (Applied Biosystems). Only sequences that could be shown to be derived from independent templates were

analyzed (12).

Phylogenetic analysis

A consensus sequence for each sample was generated with forward and reverse sequences using default assembly parameters on CodonCode Aligner software (CodonCode Corporation). Each consensus sequence was aligned with HXB2 reference HIV-1 sequence from the Los Alamos National Laboratory HIV sequence database using BioEdit software. Aligned sequences were trimmed to the same length for phylogenetic tree generation. Genetic distances were calculated, and neighbor-joining trees (81) were generated using a maximum composite likelihood algorithm and default parameters using MEGA7 software (82) (Molecular Evolutionary Genetics Analysis Program). The conclusions were not sensitive to the method of tree generation, and neighbor-joining trees are shown in the figures.

Statistical analysis of clones

A statistical test was designed to see if changes in the frequency distribution of clones carrying sequence-identical replication-competent virus were significantly different between time points or if they could be attributed to sampling error alone. Under this null model, samples from two different time points are drawn from the same underlying distribution. Physiologically, this corresponds to a scenario in which the clonal composition of the latent reservoir does not change over time. In order to construct a null distribution of data for this model, data from two time points were aggregated and re-partitioned randomly while all margins were fixed (implemented using the R package *vegan*, Oksanen et al.). To test whether the observed data supported a more extreme difference in proportions than the re-partitioned data, the likelihood ratio test statistic was calculated for the observed data and the distribution of re-partitioned data under a multinomial model. The likelihood ratio test statistic T was derived by finding the maximum likelihood parameter estimate vector \hat{p} for a multinomial model with the combined clone size data (n_{1+2}) and a multinomial model with separated data (n_1, n_2) , and then calculating their respective likelihoods.

$$T = -2\log\left(\frac{L(n_{1+2}|\hat{p}_{1+2})}{L(n_1|\hat{p}_1)L(n_2|\hat{p}_2)}\right)$$

P-values correspond to the proportion of random partitions with statistic *T* were at least as large as that of the true observation. This test is equivalent to a Fisher's exact test when the permuted matrices are ordered by the above statistic.

Results

CD4⁺ T cells containing replication-competent virus can proliferate in response to T cell receptor (TCR) activation and cytokine treatment

The immune system maintains normal levels of T cells in part through a process of homeostatic proliferation. For CD4⁺ T cells, the γ c-cytokine IL-7 is an important stimulus for homeostatic proliferation *in vivo* (39, 40). A previous study evaluated the role of IL-7-driven proliferation in HIV-1 reservoir stability and demonstrated relationship between plasma IL-7 concentration and reservoir size (13). Bosque et al. used a primary cell model of HIV-1 latency to demonstrate that latently infected central memory T cells could proliferate in the presence of IL-7 without viral reactivation (24). To explore the stimuli and conditions associated with proliferation of infected cells *in vivo*, we purified resting CD4⁺ T cells from 10 HIV-1-infected donors on ART and stained the cells with carboxyfluorescein succinimidyl ester (CFSE) dye. The cells were then treated with anti-CD3/CD28 antibodies or with an optimal concentration of IL-7 (79) for 7 days in the presence of antiretroviral drugs (Figure 1 a). IL-2 was included in all of the cultures to maintain cell viability and match the conditions described by Bosque et al. (24). Most cells proliferated in response to anti-CD3/CD28 antibodies, while proliferation induced by IL-7 was more limited (Figure 1 b). We also examined the activation status of cells cultured for 7 days with anti-CD3/CD28 or IL-7 by flow cytometry. Cells were stained for CD69, CD25 and HLA-DR. With anti-CD3/CD28 stimulation, most cells were positive for CD25, while only 20% of the cells treated with IL-7 were positive for CD25 (Figure 1 b).

The cells receiving each stimulus were then sorted based on whether they had proliferated in response to anti-CD3/CD28 or IL-7. This allowed us to examine the properties and fate of infected cells that had recently gone through the cell cycle. We sequenced the T cell receptors (TCRs) in the sorted CFSE low cell populations that proliferated in response to each treatment and compared the sequences to those in the resting T cell population. With anti-CD3/CD28 stimulation, the proportions of cells with particular TCRs

remained the same as in unstimulated resting CD4⁺ T cells ($P>0.001$), while some clones achieved a higher frequency in the population that proliferated in response to IL-7 compared to that in unstimulated resting CD4⁺ T cells ($P<0.001$) (Figure 1 c). To explore the non-uniform expansion induced by IL-7, we then analyzed IL-7 receptor (CD127) expression on resting CD4⁺ T cells from infected individuals and found that 90% of the cells expressed CD127 (Figure 1 d). This observation indicates that not all resting CD4⁺ T cells are able to proliferate in response to cytokines, which may provide a partial explanation for the preferential expansion of certain clones in response to IL-7 (Figure 1 c). In any event, the sorting of cells that had proliferated in response to anti-CD3/CD28 or IL-7 allowed us to directly examine the clonal expansion of HIV-1-infected cells.

We next asked whether either stimulation induced rapid virus release from freshly isolated resting CD4⁺ T cells. We collected culture supernatants from resting CD4⁺ T cells from 10 infected individuals after 7 days of stimulation with media alone, anti-CD3/CD28, or IL-7. Anti-CD3/CD28 induced virus production, as measured by HIV-1 mRNA in the supernatants. IL-7 treatment induced detectable HIV-1 mRNA in the supernatant of cells from 5 out of 10 infected individuals but the HIV-1 mRNA levels for those patients were at least 2 logs lower than those observed with anti-CD3/CD28 (Figure 1 e). The finding that latently infected CD4⁺ T cells treated with IL-7 can proliferate with little or no virus production suggests that homeostatic proliferation induced by cytokines could potentially expand the latent reservoir without exposing the infected cells to immune clearance. Anti-CD3/CD28 induced much higher levels of T cell proliferation and latency reversal.

Most infected cells harbor defective proviruses that may not interfere with clonal expansion (37, 38). To determine whether cells harboring replication-competent HIV-1 genomes can proliferate in response to these stimuli, we plated the sorted cells that had proliferated in response to anti-CD3/CD28 or IL-7 in a limiting dilution quantitative viral outgrowth assay (QVOA) (Figure 1 a). In this assay, the cells are stimulated with PHA and γ -irradiated allogeneic peripheral blood mononuclear cells (PBMC) to reverse latency as previously described (41, 42). Infectious virus particles released following reversal of latency are detected by adding MOLT4/CCR5⁺ cells to the culture. These cells lack class II MHC expression and do not cause allogeneic stimulation of patient cells (42). However, they are highly susceptible to infection and allow exponential growth of infectious virus released from patient cells. With this assay, we detected viral

outgrowth by p24 ELISA assay of supernatants from cultures of unstimulated resting CD4⁺ T cells or cell populations that had proliferated in response to stimulation with either anti-CD3/CD28 or IL-7 (Figure 1f). The frequencies of cells that were able to produce replication-competent virus were similar in all three cases (Figure 1 f). Thus cells harboring replication-competent virus can proliferate in response to either TCR stimulation or cytokines, survive for at least 7 days, and retain the ability to produce infectious virus upon subsequent stimulation.

In the same experiment, cell populations that had proliferated in response to either anti-CD3/CD28 stimulation or cytokine treatment were also plated in the QVOA without additional PHA stimulation. Viral outgrowth was observed in cultures set up with MOLT-4 cells and cells that had proliferated in response to anti-CD3/CD28 without another round of PHA activation, suggesting that CD4⁺ T cells carrying replication-competent provirus can proliferate with anti-CD3/CD28 stimulation and continue to produce virus for at least 7 days. However, no viral outgrowth was observed in cultures set up with cells that had proliferated in response to IL-7 unless PHA and irradiated allogeneic PBMC cells were added (Figure 1 f). This result suggests that the concentrations of cytokines used in this culture assay were sufficient to induce proliferation of some resting CD4⁺ T cells without latency reversal. The progeny cells could produce virus with additional stimulation. We have previously shown that CD4⁺ T cells harboring replication-competent provirus can proliferate in response to global T cell activation without producing virus while retaining the ability to do so upon subsequent stimulation (18, 37). Thus both antigen and cytokines provide a potential explanation for the presence of expanded cellular clones in the latent reservoir.

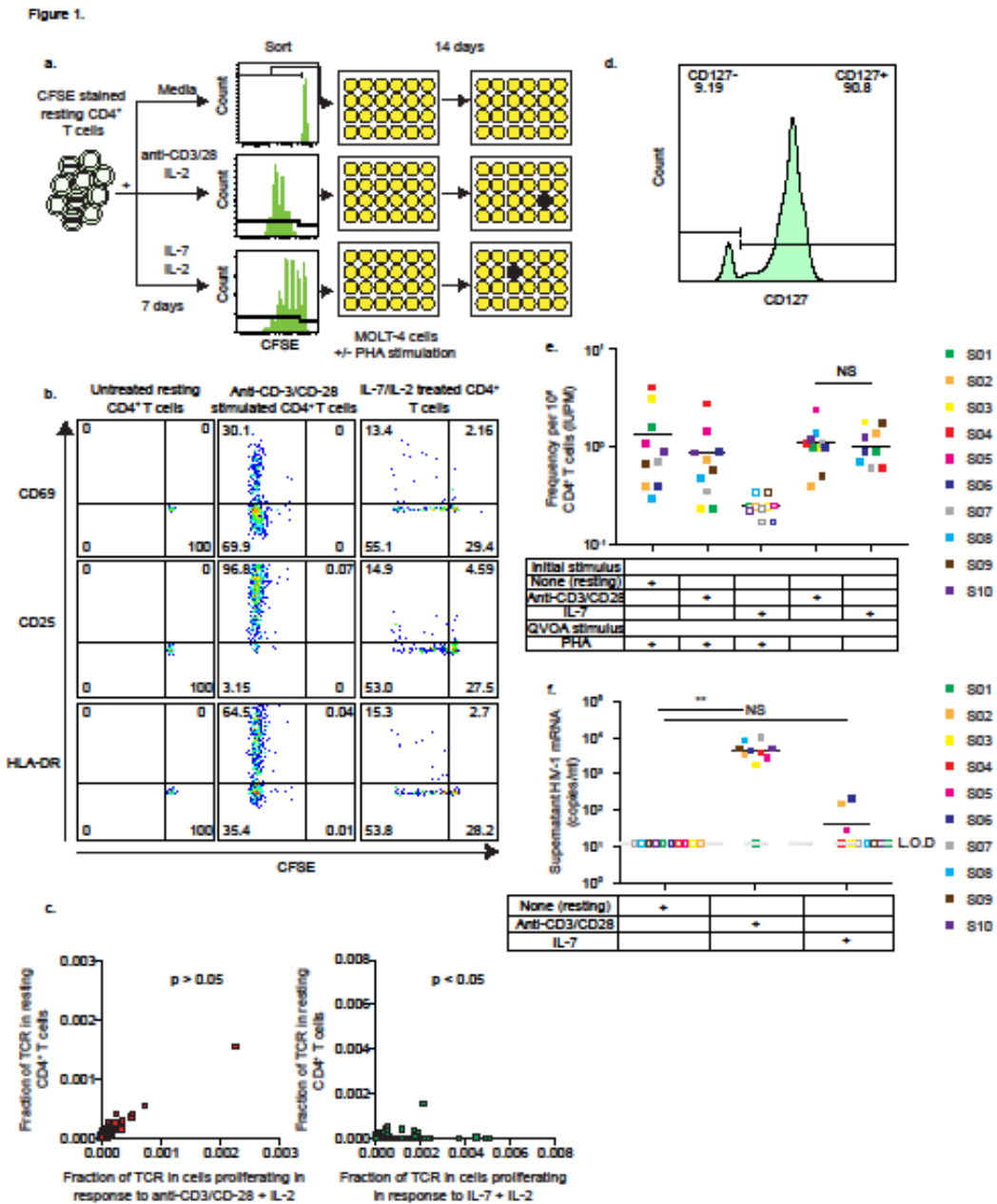


Figure 1: Proliferation of infected cells in response to TCR stimulation and cytokines. (A) Experimental setup with assay time course. Resting CD4⁺ T cells were isolated from participants on ART; stained with CFSE; and then cultured for 7 d with media alone, cultured with anti-CD3/CD28, or treated with IL-7. On day 7, cells that had proliferated in response to anti-CD3/CD28 or IL-7 were isolated based on CFSE dilution. Half of the sorted cells were then plated in a limiting dilution QVOA with PHA and irradiated allogeneic PBMCs. The other half of the cells were plated at the same dilutions without PHA or irradiated allogeneic PBMCs. After 24 h, PHA was removed and MOLT-4/CCR5⁺ cells were added to all culture wells to expand virus released from infected cells. On day 20, a p24 ELISA was performed to quantify viral outgrowth. Cells treated with media alone were cultured without sorting.

(B) Activation marker expression and proliferation induced by anti-CD3/CD28 and IL-7 stimulations. Resting CD4+ T cells were stained with CFSE before stimulation. CFSE dilution and activation marker expression were quantitated by flow cytometry 7 d after stimulation.

(C) TCR sequence analysis. TCRs of cells that proliferated with anti-CD3/CD28 stimulation or IL-7 stimulation were sequenced, and the percentage of each TCR was then calculated in each sample.

(D) Resting CD4+ T cell expression of IL-7 receptor (CD127). Freshly isolated resting CD4+ T cells were stained with CD127 to quantify IL-7 receptor expression level before any treatment.

(E) Induction of virus production by anti-CD3/CD28 and IL-7. Resting CD4+ T cells from individuals on ART (n = 10) were left untreated or simulated with anti-CD3/CD28 or IL-7 for 7 d. HIV-1 RNA levels in culture supernatants were measured by qRT-PCR. **P < 0.01. L.O.D., limit of detection; NS, P > 0.05.

(F) Frequency of latently infected cells that proliferated in response to anti-CD3/CD28 or IL-7 as measured by QVOA. Sorted cells were analyzed by QVOA with or without an activating stimulus (PHA and allogeneic PBMCs). The frequency of cells producing replication-competent virus was determined by limiting dilution statistics 14 d later.

Some expanded clones harboring replication-competent virus persist overtime while others wax and wane

Three recent studies showed that expanded cellular clones containing replication-competent HIV-1 are common in infected individuals (17-19). However little is known about the dynamics of these clonal populations. To examine whether these clones persist, we recovered the infectious virus from 8 treated individuals at 2 or 3 time points spanning 2 to 3 years (Figure 2 a). Limiting dilutions of resting CD4+ T cells were subjected to stimulation in the QVOA with the T cell mitogen PHA and γ -irradiated allogeneic PBMC. MOLT-4/CCR5+ cells were added on day 2 of the culture to expand virus released from cells in which latency was reversed, and the culture supernatants were tested for virus production by p24 ELISA on day 14 (42). We amplified the highly variable V3-V4 region of the *env* gene by RT-PCR from viral RNA in the supernatants of all p24+ wells from the QVOA. As expected from the limiting dilution format of the QVOA, sequences from individual p24+ wells should represent independent isolates of replication-competent virus. Sequences from each individual were compared by phylogenetic analysis. All 8 individuals had one or more sets of independent isolates with identical *env* sequences at 2 or 3 time points (Figure 2 a). To determine whether these isolates with identical *env* sequences were identical throughout the genome, a previously described clonal prediction score was used (83). The *env* amplicon had a clonal prediction score of 96, indicating that 96% of the sequences identical in this region are identical throughout the entire HIV-1 genome. In addition, we previously established using full genome sequencing that a subset of these sequences obtained at the first time point were identical throughout the entire HIV-1 genome (Figure 2 a) (18). Phylogenetic analysis

established that identical proviruses in these patients reflect expanded cellular clones rather than infection of a large number of cells by a dominant viral species (18). Therefore each set of identical *env* sequences is very likely to represent a clonal population of infected cells derived from a single initially infected cell by extensive *in vivo* proliferation.

Longitudinal sampling over a 1-3 year time span allowed us to address the question of whether clones harboring replication-competent virus persist over time. In 7 out of 8 individuals, we observed sequences that were present and prevalent at one time point at other time points (Figure 2 a, b), suggesting some cellular clones persisted on a time scale of years and comprised a substantial fraction of the total population of resting CD4⁺ T cells with replication competent proviruses over these time periods. However, in 7 out of 8 individuals, we also found clonal populations carrying different replication-competent viruses at time point 2 and time point 3 that were not present at time point 1 (Figure 2 a, b). In addition to the appearance of new clones, we also observed the disappearance of other clones. In subject S01, one large expanded clone was only observed at time point 1 and then disappeared, while another expanded clone appeared and was only seen at time point 2 (Figure 2 a, b). The same dramatic appearance and disappearance pattern was observed in subject S04 (Figure 2 a, b). Of all the sequences collected, 65.6% were seen only at one time point. Of 17 clones observed at two or more time points, 10 clones showed an increasing frequency over time while 7 clones decreased in frequency over time. Overall these results are consistent with a homeostatic processes in which individual clones increase and decrease in frequency while the size of the total pool of latently infected cells decreases only very slowly (1, 7, 8). Due to the low frequency of cells harboring inducible replication-competent proviruses, the number of infected cells sampled at any given time point is limited. We therefore analyzed whether a difference in observed clone frequencies between time points within the same patient could be attributed to sampling error alone (Figure 2b). In most comparisons between pairs of time-points, the observed difference in clone frequencies was highly significant, supporting the notion that the difference in clone frequencies cannot be accounted for by sampling alone (Figure 2b). These findings demonstrate that clonally expanded cells harboring replication-competent virus wax and wane on a time scale of years. Our results do not support a process of continuous expansion.

Figure 2a.

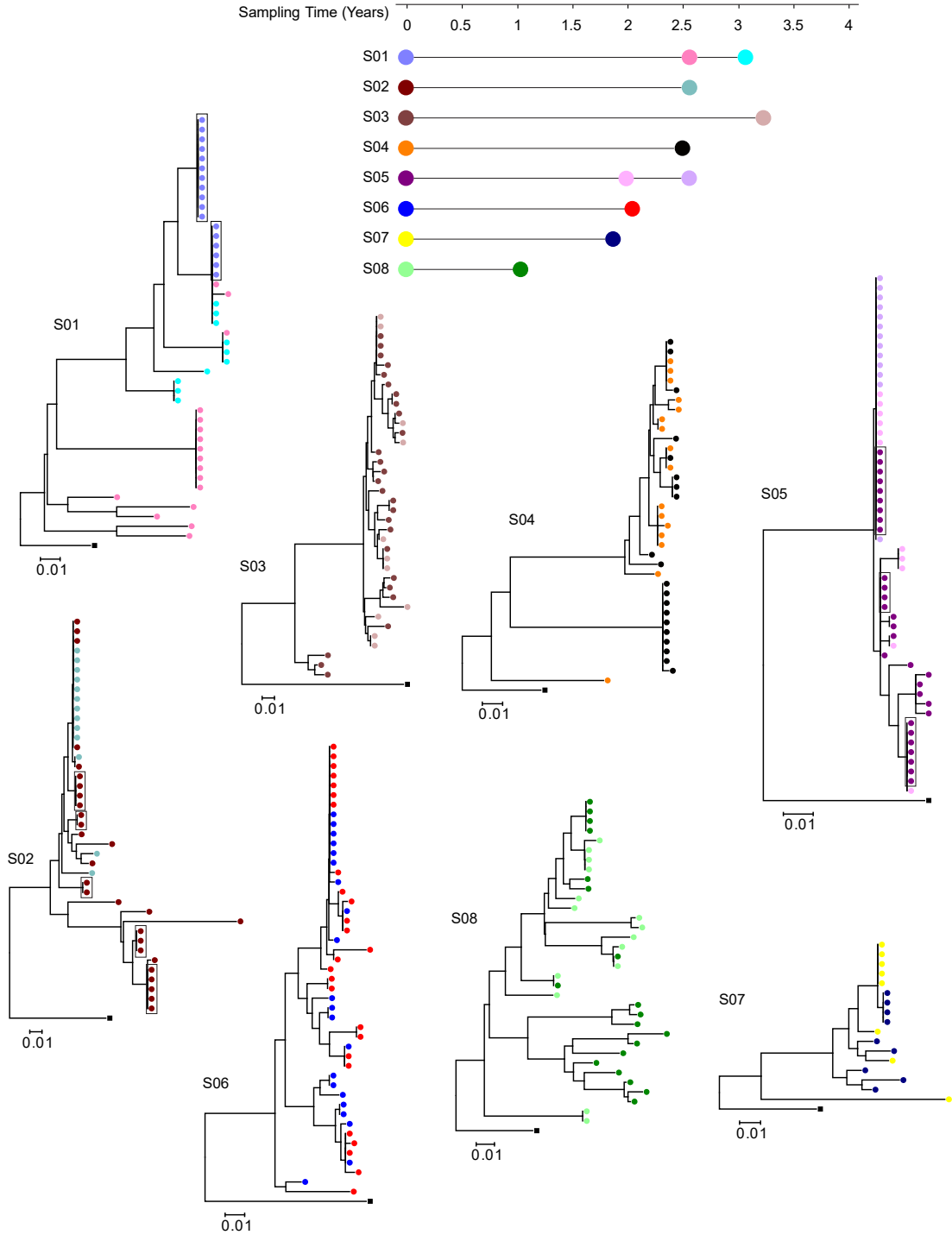


Figure 2b.

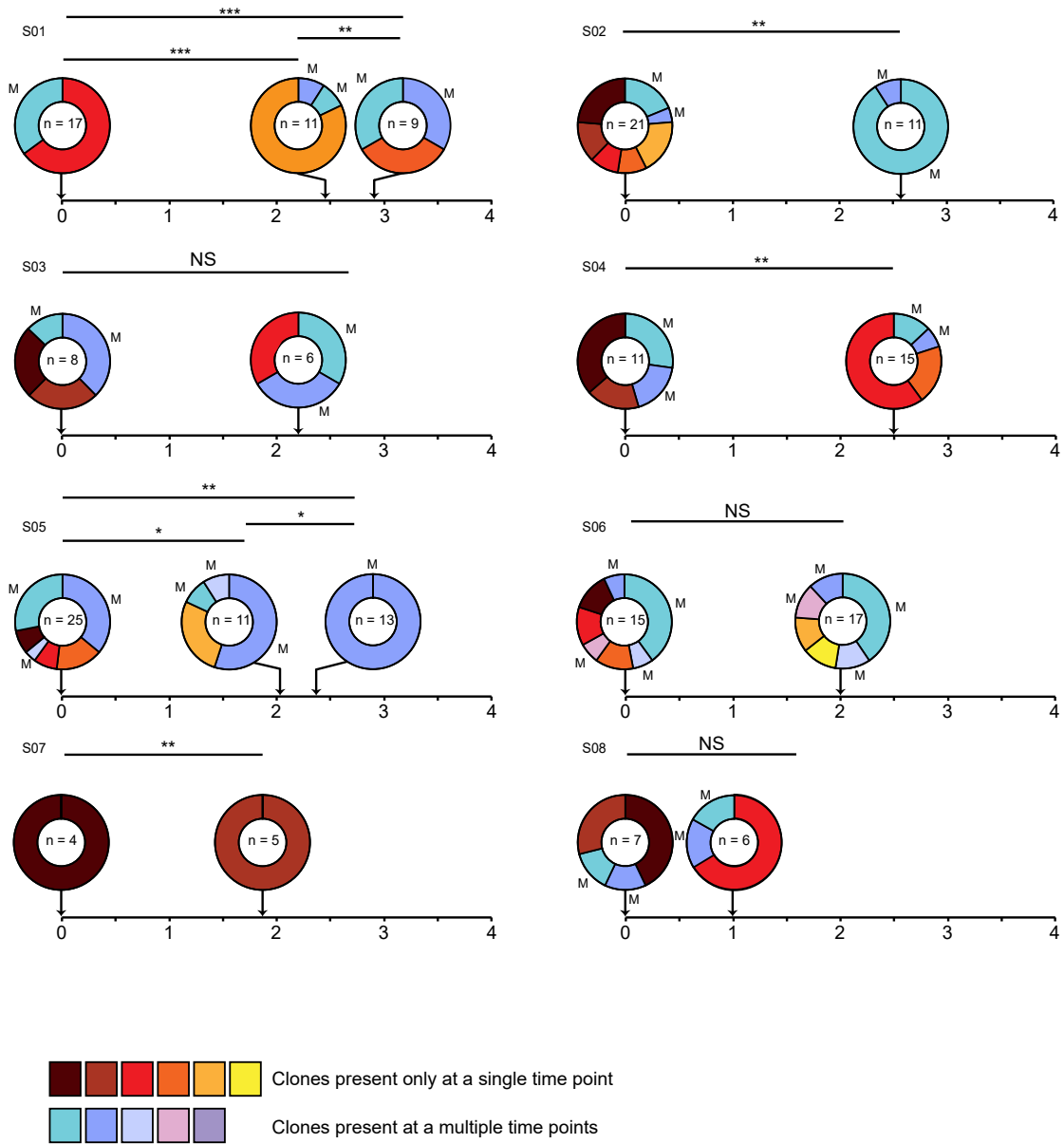


Fig. 2. Expanded clones carrying replication-competent HIV-1 emerge and wane over time.

(A) Phylogenetic trees of *env* sequences of independent isolates of replication-competent virus from eight subjects on ART (S01–S08) are shown. Sequencing was performed on genomic viral RNA in supernatants of p24+ wells. Different colors correspond to viruses recovered from different time points as indicated under the time line. Groups of identical sequences are indicated by symbols present on the same vertical “rake.” Sequences for the first time point were included in a previous study (18). Sequences that were previously shown to be identical by full-genome sequencing are grouped in boxes (18). The time scale indicates time in years from study entry. All patients were on suppressive ART for >6 mo before study entry. Black squares indicate the reference sequence HXB2.

(B) Dynamics of expanded clones containing replication-competent HIV-1. Each pie figure shows how all of the replication-competent viruses (*n*) collected at a specific time point (shown on the x axis) are divided into clonal populations, with distinct colors representing different clones. Clones marked by M were identified at multiple time points. Starred lines indicate samples that are significantly different according to a test for difference in clone proportions when the null model is a random partition of the aggregated samples (Materials and Methods) (**P* < 0.05; ***P* < 0.01; ****P* < 0.001; NS, *P* > 0.05).

Clonal populations of free plasma virus change overtime

To provide further insight into the dynamics of expanded cellular clones carrying replication-competent HIV-1, we analyzed residual viremia in patients on suppressive ART over time. Most of the defects found in HIV-1 proviruses are major defects that would preclude the production of virus particles (37, 38, 44). Therefore, the dynamics of the cells that produce the residual viremia are likely to reflect the dynamics of cells that carry replication-competent proviruses. However, analysis of residual viremia provides additional information because virus production requires latency reversal.

Figure 3 shows phylogenetic analysis of *env* gene sequences from plasma virus and from proviruses in resting CD4⁺ T cells from a representative patient on ART. This phylogenetic tree illustrates previously described features of residual viremia, including an intermingling of plasma and cellular sequences (12), the lack of temporal structure (degree of divergence is not correlated with time of sampling) (45), the presence of predominant plasma clones (PPC) (12), and a lack of correlation between the frequency of clonal sequences in plasma and resting CD4⁺ T cells (12). All of these features are consistent with the hypothesis that a stable reservoir of HIV-1 in resting CD4⁺ T cells contributes to the residual viremia as cells in the reservoir become activated. One large clonal population was detected at time point 1 and persisted through time point 3 five months later, but very few matching proviral sequences were found. The lack of correlation between the frequency of clonal sequences in plasma and resting CD4⁺ T cells reflects the fact that most of the proviruses

in resting CD4⁺ T cells are defective and incapable of producing plasma virus (37, 38). Therefore extensive sampling is required to find the matching proviral sequences. The presence of a large clonal population in plasma reflects not only the proliferation of a clone of infected cells but also the activation of at least some of those cells, presumably by some antigen, to a degree that reverses latency.

In 4 of 8 patients sampled, we found dominant plasma virus populations as evidenced by the identical viral sequences obtained in multiple independent single genome amplifications. Interestingly, we observed the same pattern of appearance and disappearance of these plasma virus clones as we observed with proviruses in resting CD4⁺ T cells (Figure 4 a). Subject 14 was studied at 4 time points over a 2-year period. We identified one large clonal population that was first detected at time point 2, became dominant at time point 3, and persisted through time point 4, 1.2 years later (Figure 4 a, 5). Another distinct clonal population was dominant at time point 2 but was not seen in the plasma at later time points. Another distinct clonal population of plasma virus was identified only at the last time point in this patient. This study participant also had populations of clonal proviruses from resting CD4⁺ T cells. However we only found matching proviral sequences for one of the clonal plasma viruses (Figure 4 a), consistent with the fact that the vast majority of proviral sequences are defective. These results show that clonal populations of infected cells producing residual viremia wax and wane on a time scale of years. This likely reflects changes in the frequency of individual clones, as indicated by viral outgrowth studies (Figure 2). This in turn may reflect changes in the exposure to cognate antigens that could drive both proliferation and virus production.

In subject 13, we sampled plasma viruses at 4 points over a 4-year period (Figure 4 b, 5). We observed multiple distinct clonal populations of plasma viruses, the abundance of which changed over time. In subject 15, we sampled plasma viruses at 6 time points over a 4-year period (Figure 4 b). Three distinct clonal populations of plasma viruses were identified. Two populations were observed at earlier time points but not after the 3rd time point. Another population was only observed at time point 5 and time point 6 (Figure 4 b, 5). The pattern of emergence and disappearance of clonal populations of plasma virus is summarized in Figure 5. This pattern is consistent with our finding that clonal populations of replication-competent provirus wax and wane overtime and supports a model of release of virus from clonally expanded cells in the reservoir.

Figure 3.

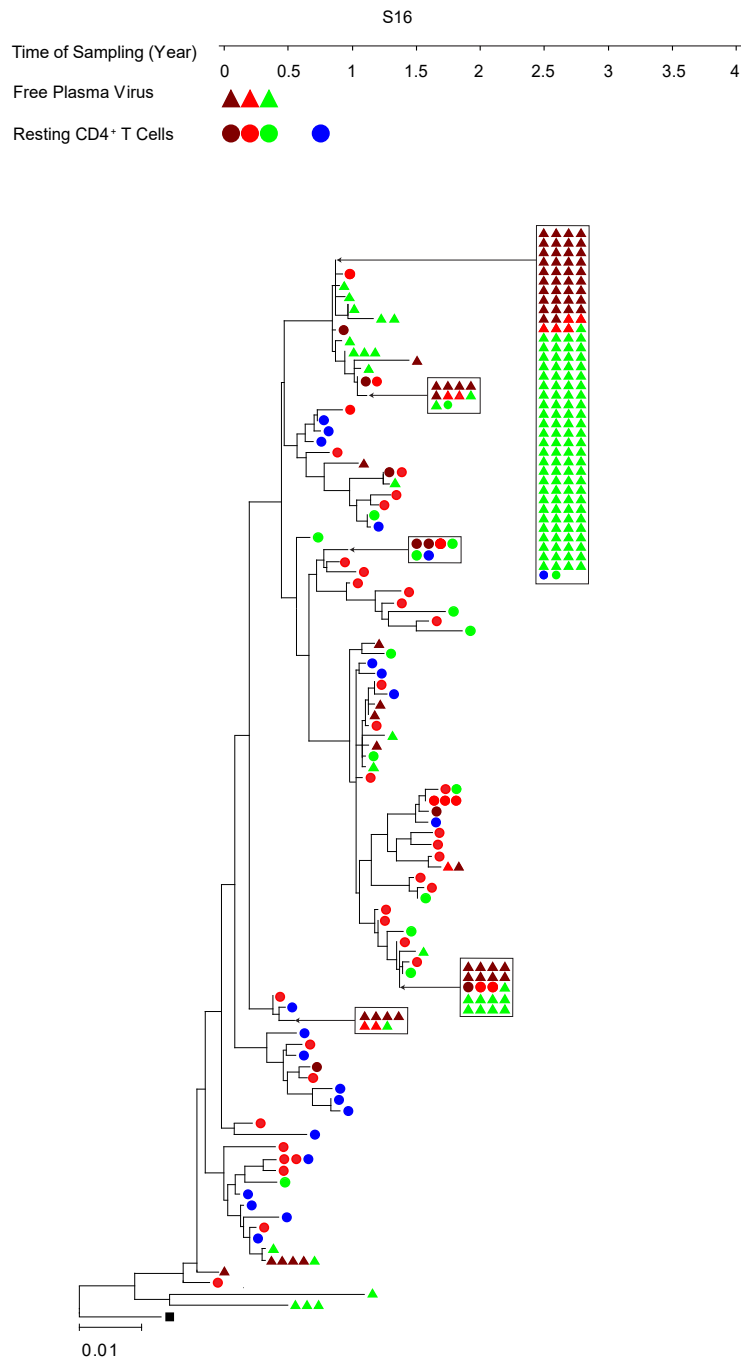


Fig. 3. Neighbor-joining phylogenetic tree constructed with env sequences from the plasma and resting CD4+ T cells from subject S16. Samples were taken at the indicated times after study entry while the plasma HIV-1 RNA level was <50 copies per milliliter. Samples were processed for analysis of HIV-1 RNA in plasma (triangles) and proviral DNA in resting CD4+ T cells (circles).

Figure 4 a.

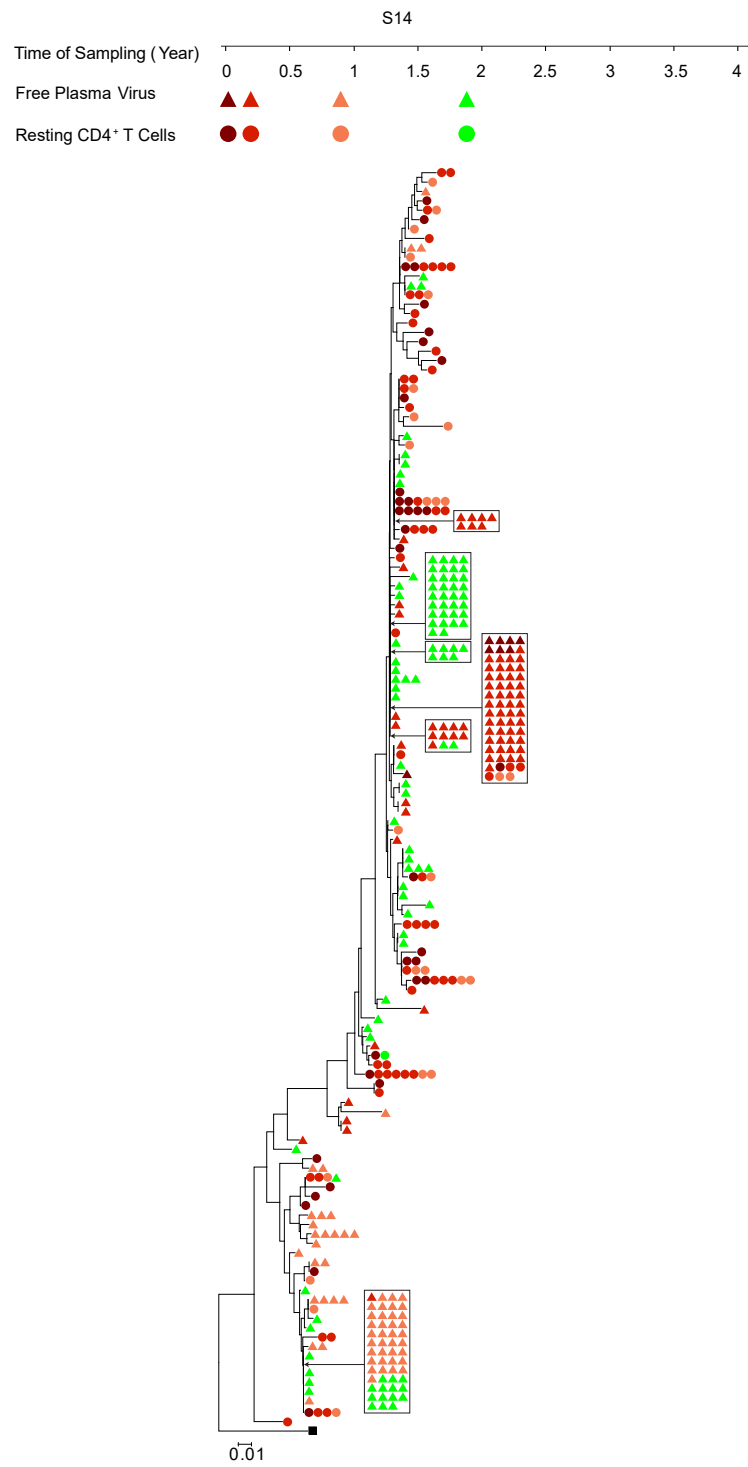


Figure 4 b.

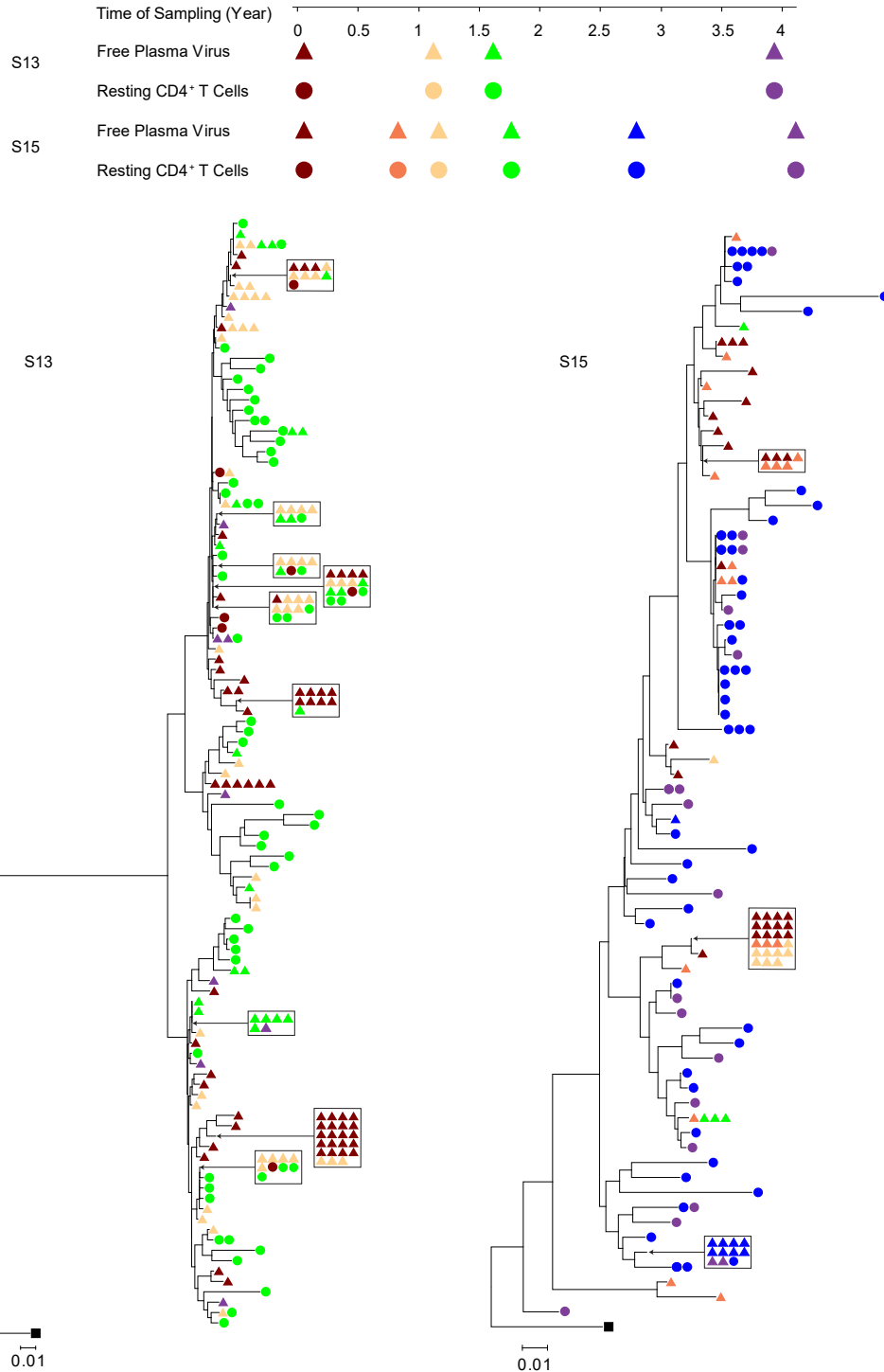


Fig. 4. Plasma virus clones wax and wane over a time scale of years. Neighbor-joining phylogenetic trees constructed with env sequences from the plasma (triangles) and resting CD4⁺ T cells (circles) from subjects S14, S13, and S15. Samples were taken at the indicated times after study entry while the plasma HIV-1 RNA level was <50 copies per milliliter.

Figure 5.

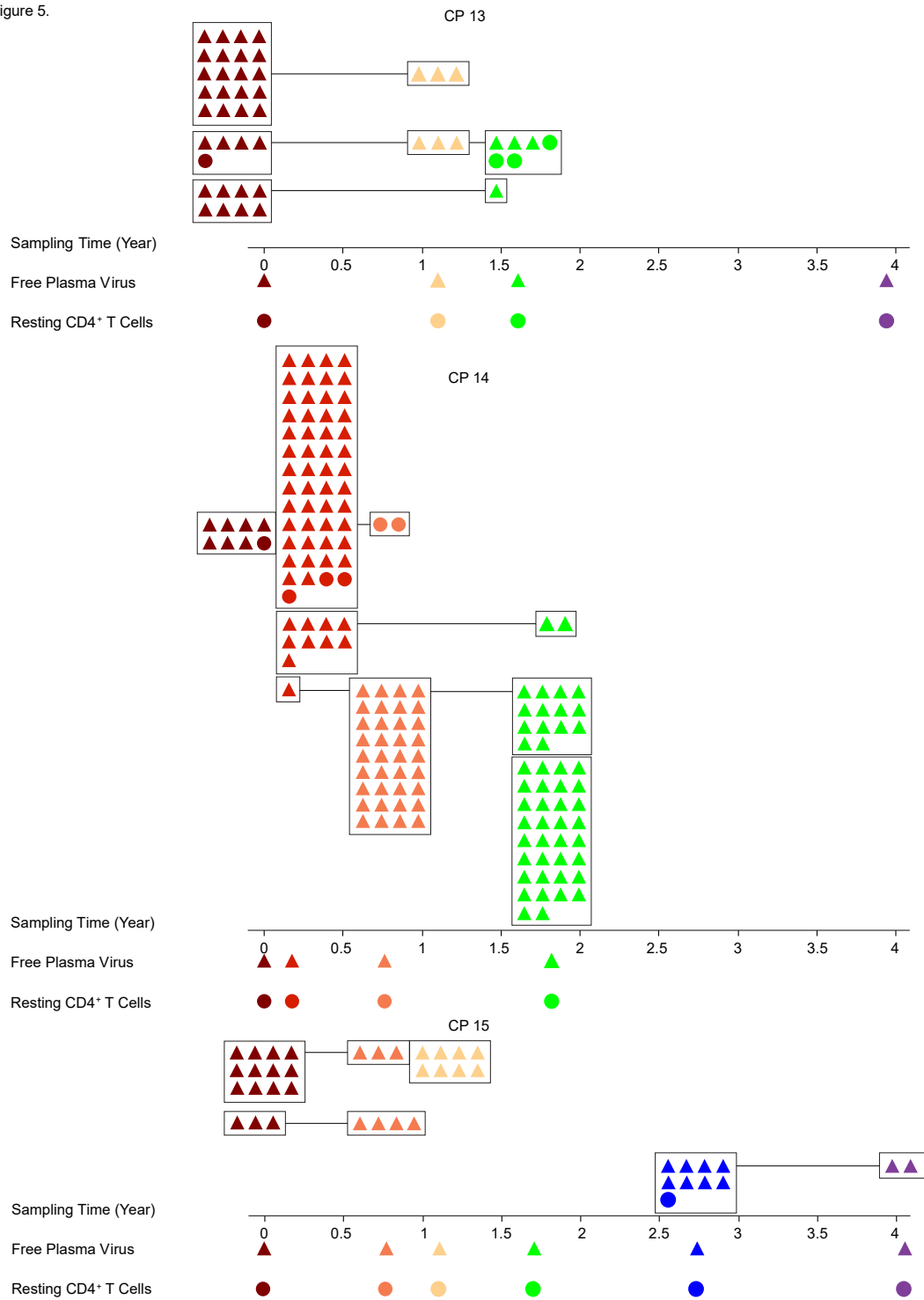


Fig. 5. Composite graph illustrating the appearance and longevity of clonal populations of free plasma virus and provirus derived from resting CD4+ T cells. Colors correspond to time of sampling and are derived directly from the corresponding phylogenies.

Discussion

The stable latent reservoir for HIV-1 in resting CD4⁺ T cells is a major barrier to cure (1). Proliferation of infected cells could explain the stability of the latent reservoir. However, some mechanisms that drive proliferation of infected cells also induce proviral expression so that infected cells can be eliminated by immune mechanisms or die from viral cytopathic effects (20, 21). Despite the fact that productively infected cells have a very short half-life (84, 85), accumulating evidence suggests that infected cells harboring replication-competent virus can undergo clonal expansion *in vivo* (16). Sequencing of plasma virus in subjects on ART provided additional evidence for clonal expansion of cells carrying replication-competent virus, as residual viremia is often dominated by identical viral sequences (11, 12). There is great current interest in understanding the stimuli driving clonal expansion.

Studies in a model system suggested that infected cells can proliferate in response to IL-7 and IL-2 without viral reactivation (79). Therefore, we examined into whether infected cells carrying replication-competent virus from patients on ART could expand through cytokine-driven homeostatic proliferation and whether clonally expanded populations persist overtime *in vivo*. We demonstrate here using patient samples that infected cells harboring replication-competent HIV-1 can proliferate through TCR or cytokine-driven mechanisms. We show that cells carrying replication-competent HIV-1 can proliferate in response to cytokine treatment and do so without producing infectious virus while retaining the ability to produce virus following a subsequent stimulation. It is worth noting that the level of proliferation induced by cytokine treatment is related to IL-7 receptor expression. IL-7 receptor α chain CD127 is expressed at higher levels in central memory and transitional memory CD4⁺ T cells but not in effector memory CD4⁺ T cells (39, 46). We have previously shown that latently infected cells carrying replication-competent proviruses can also proliferate in response to mitogen stimulation without producing virus (66). These findings are consistent with the observation of clonal expansion *in vivo* and help explain the large number of latently infected cells carrying identical intact viral sequences (18).

Although it is clear that the latent reservoir is dominated by clonal populations of infected CD4⁺ T cells, the dynamics of these populations have been unclear and could differ from those of clonal populations of infected cells carrying defective proviruses. We show here that some clonal populations of resting CD4⁺ T cells carrying replication-competent HIV-1 wax and wane *in vivo* on a time scale of years, while others persist

over the time period examined. We also demonstrate that clonal populations of plasma viruses emerge and disappear on a time scale of years in participants on ART. The observations on plasma virus suggest are consistent with the presence of expanded cellular clones and show that at least a fraction of the cells are constantly activated to produce virus. The waxing and waning of predominant plasma viral populations is likely a reflection of the underlying proliferative mechanisms that maintain the latent reservoir as well as changes in the stimuli that drive infected cells to produce virus.

Overall, these results support the hypothesis that the latent reservoir is maintained by clonal proliferation. This is important, as eradication of HIV-1 infection necessitates elimination cells carrying replication-competent latent proviruses, and the potential of these cells to undergo enormous clonal expansions makes eradication more challenging. Therefore it is important to determine the mechanisms responsible for clonal expansion of cells carrying replication-competent proviruses. The observation that expanded clones wax and wane overtime suggests that proliferation of infected cells is balanced by a significant amount of cell loss. The dynamic changes support antigen and cytokines as potential drivers of clonal expansion, but they do not support a cell autonomous proliferation driven by effects related to the site of integration, as such a mechanism would be more likely to result in progressive expansion.

Chapter Two: Evaluating the role of HIV-1 provirus in persistence of infected cells: implications for cure strategies

Introduction

A stable latent reservoir for HIV-1 in resting CD4+ T-cells precludes cure (23, 25, 76). Early studies of infected donors on suppressive ART demonstrated that a subset of these cells carrying replication-competent HIV-1 could be induced to replicate in tissue culture, comprising what we now consider the latent reservoir. However subsequent studies have revealed that a complex population of both replication-competent proviruses and defective proviruses coexist in every infected individual. Curative strategies targeting the reservoir are being tested (74, 75, 86) and require accurate, scalable reservoir assays. The development of assays that measure HIV-1 persistence has been invaluable in furthering our understanding of the impact of ART on viral replication and the nature of the latent reservoir. However, current methods have several limitations and the quantification of the latent reservoir remains challenging. The reservoir was defined with quantitative viral outgrowth assays (QVOAs) for cells releasing infectious virus following one round of T-cell activation (86). However, QVOAs and newer assays for cells producing viral RNA or virions may underestimate reservoir size because studies have demonstrated that additional proviruses are induced following more rounds of activation (66). QVOA allows quantification of replication-competent proviruses, but it is labor and time consuming, which makes them impractical for large cohort studies. Given the complexity of the QVOA, most studies rely on PCR-based assays to detect proviral DNA regardless of transcriptional status. PCR-based assays that measure HIV-1 DNA have a higher throughput, but the clinical relevance of these assays is unclear, as these PCR-based assays would miss proviral defects outside of the region amplified. Given that defective proviruses greatly outnumber intact proviruses in most chronically treated individuals, these PCR-based assays could overestimate the size of the latent reservoir. Additionally, infected cells carrying intact versus defective proviruses may respond differently to a given intervention. Therefore, total HIV-1 DNA data could be misleading.

We describe a novel approach that separately quantifies intact and defective proviruses and show that the dynamics of cells carrying intact and defective proviruses are different in vitro and in vivo, a finding with implications for targeting the intact proviruses that are a barrier to cure.

Materials and Methods

Study participants

Characteristics of study participants are given in Table 1. The Johns Hopkins Institutional Review Board and the UCSF Committee on Human Research approved this study. All participants provided written consent prior to enrollment. Except where indicated, participants were HIV-1 infected adults on suppressive ART with undetectable plasma HIV-1 RNA levels (< 50 copies per mL) for >6 months. Chronic phase (CP)-treated subjects are defined as subjects starting ART >180 days from the estimated date of infection. Acute phase (AP)-treated subjects started ART < 100 days after the estimated date of infection. For longitudinal analysis, additional peripheral blood mononuclear cell (PBMC) samples were obtained from 10 HIV-1-infected men followed in the Baltimore-Washington DC center of the Multicenter AIDS Cohort Study (MACS) (87) who had undetectable plasma HIV RNA (<20 copies/ml by Roche Taqman assay) at all semiannual study visits for 5 years or more, with no blips or missed visits. PBMC cryopreserved at visits at least 5 years apart, and viably stored as per MACS protocols, were studied. Characteristics of these 10 men are given in Table 1 (CP31-CP49).

CD4+ T-cell isolation

Peripheral blood mononuclear cells (PBMCs) were isolated by density centrifugation using Ficoll-Paque PLUS (GE Healthcare Life Sciences; Marlborough, MA) per manufacturer's instructions. Untouched total CD4+ T-cells were then enriched from PBMC using negative immunomagnetic selection via the EasySep Human CD4+ T Cell Enrichment Kit (StemCell Technologies; Vancouver, BC). In some experiments, resting CD4+ T-cells (CD4+, CD69-, CD25- and HLA-DR-) were isolated using a second negative selection step (CD25-Biotin; Anti-Biotin MicroBeads; CD69 MicroBead Kit II; Anti-HLA-DR MicroBeads, all from Miltenyi Biotec). Resting CD4+ T-cell purity was consistently >95% as assessed using flow cytometry.

Bioinformatic analysis

We constructed an alignment of 431 published (73, 88) full length proviral sequences obtained from 28 HIV-1-infected adults by single genome analysis. Of these individuals, 19 started suppressive ART during chronic

infection while 9 started suppressive ART during acute infection. 24 had prolonged suppression of viremia (>6 months) when studied, and 5 were viremic when studied (one individual was studied at two time points, before and after ART). Clinical characteristics of these individuals are given in the relevant publications (73, 88). The proportion of different types of defects in HIV-1 proviruses varies with the stage of disease at which ART is started and the level of viremia (73). For most analyses, we used sequences from patients who initiated ART during chronic infection and who had sustained suppression of viremia to below 50 copies HIV-1 RNA/ml of plasma for >6 months. These sequences (n=211) are thus representative of the most common group of infected individuals who would be eligible for cure interventions. For analyses of specific type of defects, we used all sequences in the database with that defect. For examples, for analysis of hypermutation, we used all database sequences with hypermutation (n=100) and additional hypermutated sequences obtained by single genome env sequencing. Hypermutation in the GG or GA context was confirmed using the Hypermut algorithm (89). Positions of primers for ddPCR analysis were evaluated using a sliding window analysis of two hypothetical 100 bp amplicons, scoring for lack of significant overlap (>5%) with mapped deletions in the database sequences with deletions. Sequence conservation was evaluated using separate alignments of US clade B sequences from the Los Alamos HIV sequence database.

Intact proviral DNA assay (IPDA)

A variety of experimental conditions were used in the development of the IPDA. The following is an optimized recommended procedure. In general, the IPDA is performed on DNA from 5×10^6 CD4+ T-cells. Genomic DNA is extracted using the QIAamp DNA Mini Kit (Qiagen; Hilden, Germany) with precautions to avoid excess DNA fragmentation. DNA concentrations are determined using the Qubit3.0 and Qubit dsDNA BR Assay Kit (ThermoFisher Scientific; Waltham, MA). Quantification of intact, 5' deleted, and 3' deleted and/or hypermutated proviruses are carried out using primer/probe combinations optimized for subtype B HIV-1 (Table 3). A qualified research use only (RUO) version of the primer/probe mix is available from Accelevir Diagnostics, Baltimore, MD (HIV-1 Proviral Discrimination 20x primer/probe mix). The primer/probe mix is comprised of oligonucleotides for two independent hydrolysis probe reactions that interrogate conserved regions of the HIV-1 genome to discriminate intact from defective proviruses. HIV-1 Reaction A targets the packaging signal (Ψ) which is a frequent site of small deletion and is included in many large deletions in the

proviral genome. The Ψ amplicon is positioned at HXB2 coordinates 692-797. This reaction utilizes forward and reverse primers, as well as a 5' 6-FAM labelled hydrolysis probe. Successful amplification of HIV-1 Reaction A produces a FAM fluorescence in droplets containing Ψ , detectable in channel 1 of the droplet reader. HIV-1 Reaction B targets the Rev-Response Element (RRE) of the proviral genome, with the amplicon positioned at HXB2 coordinates 7736- 7851. This reaction utilizes forward and reverse primers, as well as two hydrolysis probes: a 5' VIC labelled probe specific for wild-type proviral sequences and a 5' unlabeled probe specific for APOBEC-3G hypermutated proviral sequences. Successful amplification of HIV-1 Reaction B produces a VIC fluorescence in droplets containing a wild-type form of RRE, detectable in channel 2 of the droplet reader, while droplets containing a hypermutated form of RRE are not fluorescent. Droplets containing HIV-1 proviruses are scored as follows. Droplets positive for FAM fluorescence only, which arise from Ψ amplification, score as containing 3' defective proviruses, with the defect attributable to either APOBEC-3G-mediated hypermutation or 3' deletion. Droplets positive for VIC fluorescence only, which arise from wild-type RRE amplification, score as containing 5' defective proviruses, with the defect attributable to 5' deletion. Droplets positive for both FAM and VIC fluorescence score as containing intact proviruses (Fig. 8a.b). An important aspect of the quantitation of intact proviruses is correction for DNA shearing between amplicons that artificially reduces Q2 droplets while increasing Q1 and Q4 droplets (Fig. 8b). This can be done accurately through ddPCR analysis of a host gene, which also provides a measure of input cell number. In principle, any host gene can be used, with two ddPCR amplicons spaced at the same distance as the HIV-1 amplicons described above. As demonstrated in Fig. 3d and 3e, this approach allows for accurate correction for DNA shearing. Simultaneous quantification of DNA shearing and input human genome equivalents is performed using another aliquot of the same DNA sample. For the studies described here, oligonucleotides for two independent hydrolysis probe reactions that interrogate the human RPP30 gene (Chr.10: 90,880,081 on GRCh38) were used. A qualified RUO RPP30 primer/probe mix is available from Accelevir Diagnostics, Baltimore, MD (DNA Shearing + Copy Reference 20x primer/probe mix). In this primer/mix, the total distance between duplex reactions and individual amplicon sizes are equivalent to those of the HIV-1 proviral discrimination reactions described above. Optimal reaction melting temperatures are equivalent for all reactions. Comprehensive oligonucleotide analysis predicted no potential off-target nucleotide binding or amplification (BLASTn) and no self-dimerization, hetero-dimerization, or primer hairpin formation. RPP30

Reaction A employs a 5' 6-FAM labelled hydrolysis probe, and RPP30 Reaction B employs a 5' HEX labelled hydrolysis probe. Droplets positive for both 6-FAM and HEX fluorescence score as containing an unsheared RPP30 gene fragment, while droplets positive for only a single fluorescence score as containing part of a sheared RPP30 gene fragment. The ratio of dual fluorescent to single fluorescent droplets is used to calculate a DNA Shearing Index (DSI), and this index is applied to both genome copy number input reactions and HIV-1 proviral discrimination reactions to correct for experimentally observed DNA shearing. Droplet digital PCR was performed on the Bio-Rad QX200 AutoDG Digital Droplet PCR system using the appropriate manufacturer supplied consumables and the ddPCR Supermix for probes (no dUTPS) (Bio-Rad Laboratories; Hercules, CA). For HIV-1 proviral discrimination reactions, 700 ng of genomic DNA was analyzed in each reaction well. For DNA shearing and copy number reference reactions, 7 ng of genomic DNA was analyzed in each reaction well. Multiple replicate wells were performed for each reaction type to ensure consistent quantitation, and replicate wells were merged during analysis to increase IPDA dynamic range. The following thermal cycling program was used for all reactions, with a 2°C ramp rate: enzyme activation at 95 °C for 10 min; 45 cycles at 94 °C for 30s and 59 °C for 1min; 98°C for 10min; and then infinite hold at 4 °C. In general, parallel processing and analysis of uninfected donor CD4+ T-cells was performed for each IPDA run as a negative control while qualified JLat6.3 genomic DNA was analyzed in each IPDA run as a positive control. After correction for DNA shearing, data is expressed as proviral copies per 10⁶ CD4+ T-cells.

Cell Lines

The J-Lat Full Length Clone (clone #6.3) from Dr. Eric Verdin was obtained through the NIH AIDS Reagent Program, Division of AIDS, NIAID, NIH.

Clonal microcultures

Purified resting CD4+ T-cells from HIV-1-infected donors on suppressive ART were analyzed for proviral DNA copies using gag qPCR as previously described²³. The resulting values were corrected for gag- proviruses, and cells were plated at approximately one infected cell per well (2000-4000 total resting CD4+ T-cells) in 96-well plates. The cells were then stimulated with anti-CD3/CD28 Dynabeads (25 µl per million cells; Thermo Fisher Scientific) in RPMI containing 10% fetal bovine serum and 100 U/mL IL-2 (Novartis) for 7

days in the presence of tenofovir disoproxil fumarate (10 μ M) and emtricitabine (10 μ M). Half of the media in each well was removed and replaced with fresh media, anti-CD3/CD28 Dynabeads and antiretroviral drugs weekly for 2-3 weeks. DNA isolation was performed on cells from each well using a Quick-DNA 96 Kit (Zymo Research Corporation). 1/4th of the extracted DNA was analyzed by the IPDA to determine the type of provirus and proviral copy number in each well. The remaining DNA was used for integration site analysis and full genome sequencing.

Integration site analysis

Integration site analysis was performed on cell clones obtained from clonal microcultures using previously described linker ligation method (90-92). Sites for which both the 5' and 3' junctions were captured are shown. Cancer associations were determined as previously described (92).

Full genome sequencing

DNA was subjected to a nested limiting-dilution PCR protocol as previously described using Platinum Taq HiFi Polymerase (Life Technologies). The outer PCR was nearly full-length from HIV-1 reference genome HXB2 coordinates 623 to coordinates 9,686 and employed a touchdown-PCR protocol (72, 73). The outer-PCR wells were diluted with deionized water and a small amount of outer-PCR DNA was used for nested amplification of both *gag* and *env* to determine clonality. Clonality was determined using Poisson statistics and at dilutions that gave a high probability of clonality ($P > 0.85$); all wells that were positive for outer PCR were subjected to six inner PCRs. 1 μ l of outer-PCR DNA was used for each nested inner PCR reaction. PCR products were visualized on 1% agarose gels. The products were directly sequenced to minimize PCR-induced error, using the QIAquick Gel Extraction Kit followed by Sanger sequencing. Sequencing reads from the six overlapping nested PCRs were aligned and compared to the reference HIV-1 genome HXB2 using CodonCode Aligner software to reconstruct near full length sequences and identify defects. Hypermutation was determined by using the full-length sequence for each clone and the Los Alamos hypermut algorithm.

Results

Analysis of HIV proviral sequences

Evaluation of cure strategies requires assays that not only detect infected cells, but also determine whether the proviruses they carry are intact so that reductions in the relevant population of proviruses are apparent despite the vast excess of defective proviruses. We assembled a database of 431 published (73, 88) full genome HIV-1 sequences obtained by single genome analysis from 28 HIV-1-infected adults (see Methods) and used it to determine how well PCR assays meet these requirements. Consistent with previous reports (73, 88, 89, 93, 94), only 2.4% of proviruses from treated individuals were intact (defined here as lacking overt fatal defects). The remaining 97.6% had fatal defects including deletions and/or G to A hypermutation (Fig. 6a). Because deletions were large (encompassing on average 49.6% of the genome) and because hypermutation altered start codons and/or introduced multiple stop codons in most ORFs (73, 92), most defective proviruses had defects affecting most HIV-1 genes (Fig. 6b). For example, most defective proviruses (80-97%) had defects in the transcriptional activator Tat (Fig. 6b) and are unlikely to be efficiently transcribed after latency reversal. Thus, cure intervention dependent on viral gene expression (30, 31, 95, 96) may affect cells with intact and defective proviruses differently. Unfortunately, standard PCR assays use short subgenomic amplicons in conserved regions (Fig. 6c,d) and do not distinguish intact and defective proviruses. Deletions occur throughout the genome (Fig. 6e) affecting the fraction of proviruses detected (Fig. 6f) and the fraction of detected proviruses that are intact (Fig. 6g). Importantly, for most standard PCR assays, <10% of the detectable sequences are intact (Fig. 6g). For widely used assays targeting gag, only 6.6% of detected sequences are intact (Fig. 6g). Cells carrying these proviruses are hence less likely to be eliminated by “shock and kill” strategies. Importantly, the efficacy of a cure intervention causing a selective one log reduction in intact proviruses would not be readily detected by standard PCR assays but would be easier to detect with an assay selective for intact proviruses (Fig. 6h).

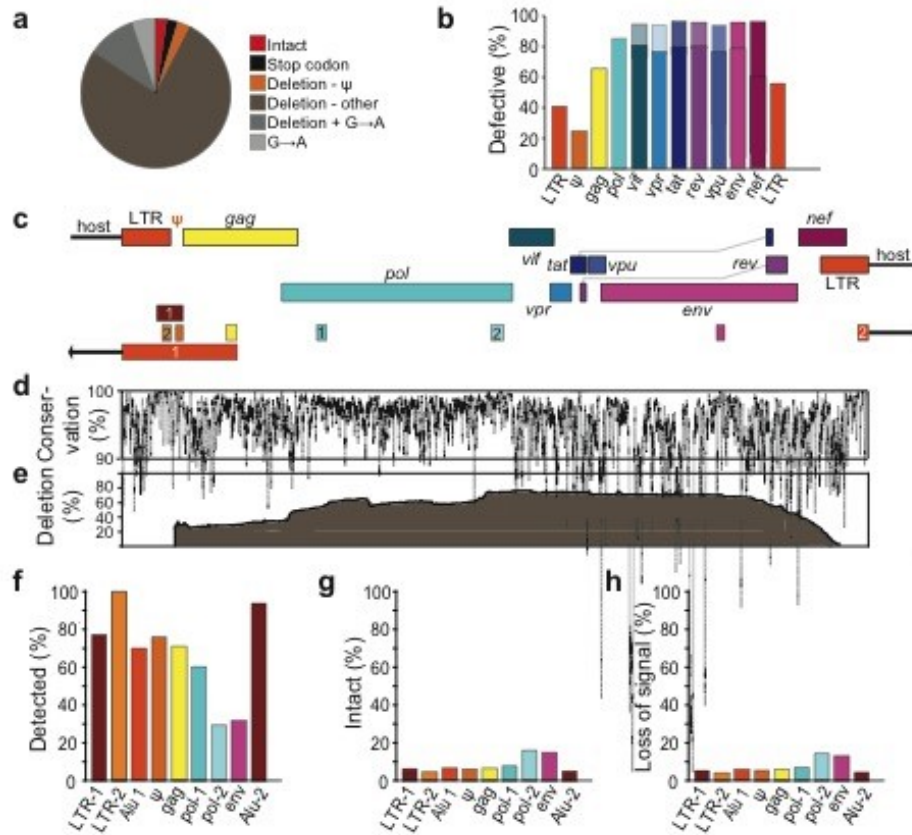


Fig. 6: Standard DNA and Alu-PCR assays predominantly measure defective proviruses.

(A) Landscape of proviruses persisting in individuals on suppressive ART as detected by full length, single genome analysis of proviruses in CD4+ T cells. Defects include internal stop codons, deletions not attributable to normal HIV-1 length polymorphisms, and APOBEC3G/F-mediated hypermutation (G→A). Most deletions were large except for those in the packaging signal (ψ)/major splice donor site. Hypermutation occurred with or without deletions. Proviruses lacking deletions, hypermutation, and internal stop codons are termed intact but may harbor minor defects affecting viral fitness. Analysis based on 211 full genome sequences from individuals initiating ART during chronic infection. The proviral landscape in patients starting ART during acute infection is also dominated by defective sequences, with a slightly higher fraction showing hypermutation.

(B) Fraction of defective sequences with inactivating defects in the indicated genes or elements. Protein-coding genes were considered defective if any of the following are present: mutated start codon, internal stop codons, frameshifts, or insertions or deletions not representing common length polymorphisms. Splice donor and acceptor site mutations are also present in many sequences, and, if included, would further increased the fraction of defective sequences for genes requiring splicing (lighter shaded portions of the bars for spliced genes). LTR sequences were considered defective if mutations in the NF κ B sites and/or deletions were present.

(C) Positions of amplicons used in standard DNA and Alu-PCR assays (bottom) relative to HIV-1 genome map (top). Numbers distinguish distinct assays targeting the same region. Alu PCR assays 1 and 2 amplify host genomic sequence (arrows) in addition to the indicated regions of the provirus.

(D) Conservation of nucleotide sequence across the genome based on US clade B sequences in the Los Alamos HIV Sequence Database (<https://www.hiv.lanl.gov/>). Plotted as % of sequences matching the consensus at each nucleotide.

(E) Position of internal deletions across the HIV-1 genome. Plotted as % of total sequences from treated patients that are deleted at the indicated nucleotide. Terminal deletions preclude integration and are not

seen. Internal deletions in the 5' LTR are not evaluable because the full genome sequencing methods do not capture this region.

(F) Percent of all proviruses that are amplified by the indicated assay. Based on absence of overlap between deleted regions and the relevant amplicons.

(G) Percent of the proviruses detected by the indicated assay that are intact by the above criteria.

(H) Percent loss of assay signal following a selective 10-fold reduction in intact proviruses. For panels f-h, analysis is based on sequences from the most common group, individuals starting ART during chronic infection (n=211 sequences from 19 patients).

Development and validation of intact proviral DNA assay (IPDA)

Interrogating individual proviruses simultaneously at multiple positions could differentiate intact from defective proviruses. Analysis of full genome sequences revealed that two strategically placed amplicons in the packaging signal (Ψ) and *env* regions could identify >90% of deleted proviruses as defective (Fig. 7a). Requiring that individual proviruses give amplification for both Ψ and *env* amplicons dramatically reduces PCR overestimate of reservoir size. The remaining overestimate is due largely to hypermutated proviruses (Fig. 6a). Among proviruses with statistically confirmed (89) G to A hypermutation, 73% had mutations in the GG to AG context. Most also had GA to AA mutations. 27% had only GA to AA hypermutation, but most of these also had deletions that would identify them as defective. Therefore, we developed a way to distinguish intact proviruses from those with the common GG to AG hypermutation pattern. We identified a conserved region within the Rev response element (RRE) that contains adjacent consensus sites (TGGG) for responsible enzyme, APOBEC3G (97, 98) (Fig. 7b-e). Of sequences with GG to AG hypermutation, 97% had one or more mutations in this region (Fig. 7c,e), with 13 distinct patterns (Fig. 7f). Allelic discrimination probes targeting this region were developed and tested using a set of mutant plasmids each carrying one of the 13 sequence patterns in quantitative PCR (qPCR) and digital droplet PCR (ddPCR) studies to validate a probe combination that correctly identified 95% of the hypermutated sequences as defective (Fig. 7f). The above analyses allowed design of a simple, rapid multiplex ddPCR assay that distinguishes deleted and/or hypermutated proviruses from intact proviruses using two PCR amplicons and hypermutation discrimination probes (Fig. 8a,b). Genomic DNA (gDNA) is isolated using an optimized method to minimize DNA shearing between targeting regions (see below) and partitioned into nanodroplets such that individual droplets rarely contain >1 provirus ($P = 0.00416$). Proviruses within droplets are analyzed simultaneously at the Ψ and *env* regions via multiplex PCR, with the *env* PCR also discriminating hypermutated proviruses. Intact proviruses give

amplification at both regions (Fig. 8a,b). The number of intact proviruses per 106 cells is calculated using separate amplification of a cellular gene (RPP30) after correction for DNA shearing.

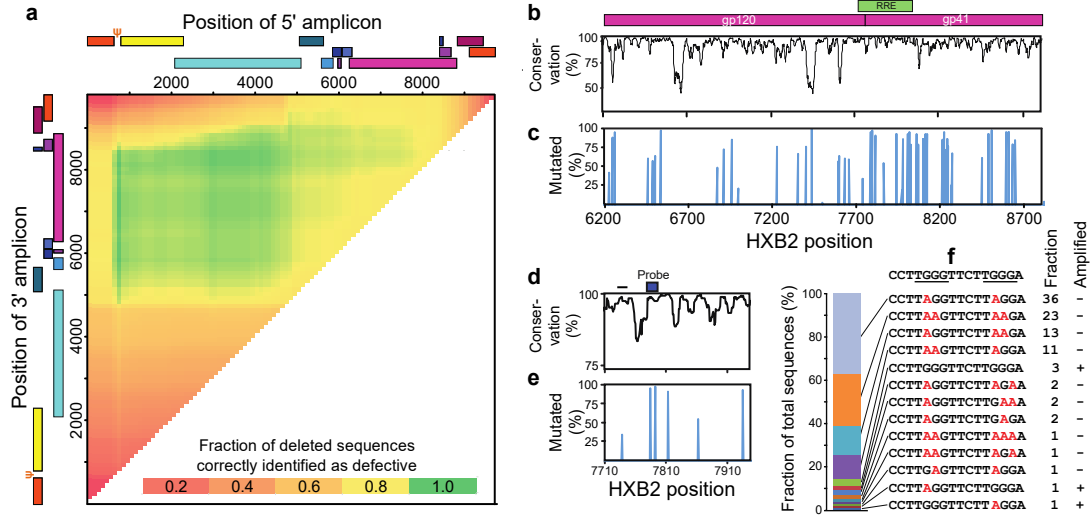


Fig. 7: Use of full genome sequences to position amplicons for distinguishing intact and defective HIV-1 proviruses.

(A) Sliding window analysis of optimal amplicon positioning. Analysis assumes two amplicons 100 bp in length are used to detect deletions. Starting positions of the 5' and 3' amplicons are shown on the horizontal and vertical axes, respectively, relative to the HIV-1 genome map. See Fig. 6 for color code of HIV-1 genes. Heat map color scale indicates fraction of deleted proviruses correctly identified as defective by overlap of one or both amplicons with the deletion. Optimal discrimination between intact and deleted sequences is obtained with a 5' amplicon in the Ψ region and a 3' amplicon in env. Ψ is the site of frequent small deletions and is included in larger 5' deletions. Based on 258 distinct full genome sequences in the database that contains mapped deletions.

(B) Degree of nucleotide conservation across the HIV-1 env gene based on US clade B sequences in the Los Alamos HIV Sequence Database. Conservation is plotted as percent of sequences matching the consensus sequence at each nucleotide position. The shaded area is expanded in Fig. 7d.

(C) GG→AG pattern hypermutation across the HIV-1 env gene. The percent of hypermutated proviruses that contain one or more G→A mutations within a given APOBEC3G consensus site is plotted as a function of site position. The shaded area is expanded in Fig. 7e.

(D) Sequence conservation of a region in the RRE containing two APOBEC3G consensus sites. The positions of primers (arrows) and probe (box) for the env amplicon selected for the intact proviral DNA assay are shown.

(E) Fraction of hypermutated proviruses that have one or more G→A mutations in the adjacent consensus sites in region chosen for probe binding (shaded).

(F) Summary of the hypermutation patterns found at the env probe-binding site. The prevalence of each of the 13 distinct patterns observed is indicated in the bar graph on the left and in the "Percent" column. Mutations in the APOBEC3G consensus sites (underlined) are indicated in red. Based on analysis of 93 independent hypermutated env sequences from 18 patients treated during either chronic or acute infection. Site directed mutagenesis was used to modify NL4-3 or a patient-derived proviral construct to generate plasmids containing each of these hypermutation patterns. The "Amplified" column indicates that only 5% of hypermutated sequences were amplified by the probe combinations developed to identify intact sequences. See Table S3 for details.

The specificity of this intact proviral DNA assay (IPDA) was verified using plasmid controls representing proviruses with different types of defects. These templates gave positive droplets in the expected quadrants: Q1, 3' deletion and/or hypermutation; Q4, 5' deletion. More importantly, cultured clonal populations of infected patient cells also give single quadrant patterns (see below). In contrast, uncultured polyclonal patient CD4+ T-cell populations give positive droplets in all three quadrants, allowing separate quantitation of intact and defective proviruses (Fig. 8c).

Extensive validation of IPDA reproducibility and linearity is provided in Figs. 9 and 10. An important issue is DNA shearing which is essential for droplet formation but artificially reduces the number of Q3 droplets while increasing Q1 and Q4 droplets. To control for shearing, a separate multiplex ddPCR amplification of two regions of a cellular gene (RPP30) spaced at exactly the same distance as the Ψ and *env* amplicons is done on every sample. This gives a DNA shearing index (DSI) that is used to correct raw HIV-1 ddPCR results. To validate this approach, DNA from JLat cells (99), which contain a single integrated HIV-1 genome, was subjected to different amounts of shearing and analyzed by ddPCR for HIV-1 and RPP30. Regardless of the degree of shearing, the DSI was similar for HIV-1 and RPP30 indicating that RPP30 shearing can be used to correct for HIV-1 shearing (Fig. 8d). At all levels of shearing tested, results corrected for shearing were close to the expected values of 1 copy/cell for HIV-1 (Fig. 8e) and 4 copies/cell for RPP30 (JLat cells are tetraploid for this gene). Thus, the assay can reliably quantitate intact proviruses in most DNA samples after correction for shearing.

Using samples of only 5×10^6 cells, we measured intact and defective proviruses with the IPDA in a large number ($n=62$) of infected individuals who had suppression of viremia on antiretroviral therapy (ART) ($n=57$) or control of HIV-1 without ART ("elite" control, $n=5$) (see Table 2 for characteristics of study participants). The mean DSI for this sample set was 0.323 ± 0.067 , well within the range for which accurate correction is possible. Intact HIV-1 proviruses were rare ($\sim 100/10^6$ resting CD4+ T cells) and greatly outnumbered by proviruses with 5' deletions and by proviruses with 3' deletions and/or hypermutation (Fig. 8f). These results provide the first direct demonstration with a method that does not depend on long PCR reaction that the proviral landscape is dominated by defective proviruses.

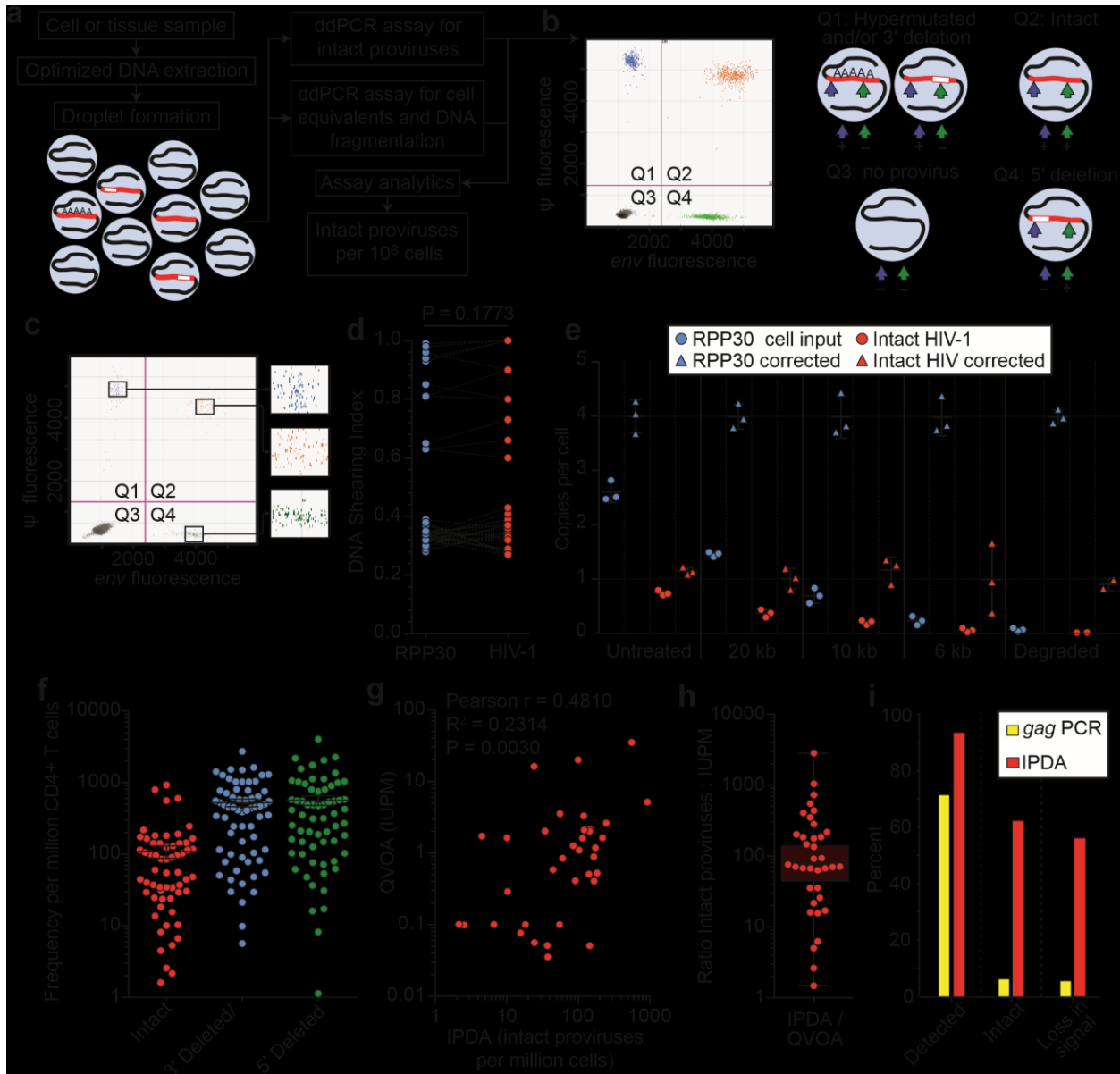


Fig. 8: Intact proviral DNA assay (IPDA).

(A) Assay schematic. Multiplex PCRs in droplets amplify Ψ and env regions. Hydrolysis probes for each amplicon are labeled with different fluorophores. A separate multiplex PCR targets two regions of the human RPP30 gene spaced at the same distance as the Ψ and env amplicons to provide cell number quantitation and DNA shearing correction. See Methods for details.

(B) Representative control ddPCR experiment using proviral constructs³⁴ with a 5' deletion (E44E11), a 3' deletion (4F11), or no defects (NL4-3). 1,000 copies each were mixed with 500ng of HIV-1 negative DNA to simulate a patient sample. Types of proviruses appearing in different quadrants are shown on the right.

(C) Representative IPDA results from a patient CD4+ T-cell sample. Boxed areas are expanded to show individual positive droplets.

(D) DNA shearing index (DSI, fraction of templates sheared between targeted regions) measured for RPP30 and HIV-1 on JLat DNA subjected to different levels of shearing.

(E) Use of DSI to correct raw ddPCR output for RPP30 and HIV. Copies/cell of RPP30 (blue) and HIV (orange) are shown before (circles) and after (triangles) correction for shearing. Shearing decreases raw droplet

counts in Q2 and increases counts in Q1 and Q4. Correction brought Q2 values for close expected values (1 copy/cell for HIV and 4 copies/cell for RPP30 (tetraploid for RPP30)).

(F) IDPA results on CD4+ T-cells from infected individuals with plasma HIV-1 RNA below the limit of detection. See Table 2 for patient characteristics.

(G) Correlation between infected cell frequencies measured by QVOA and IPDA on the same samples of CD4+ T-cells from treated patients. IUPM, infectious units per million cells.

(H) IPDA/QVOA ratios for samples from Fig. 8g.

(I) Bioinformatic comparison of standard gag PCR and IPDA with respect to % of proviruses amplified, % of amplified proviruses that are intact, and % loss in assay signal following a selective 10 fold reduction in intact proviruses induced by a curative intervention. See legend to Fig. 6f-h for details.

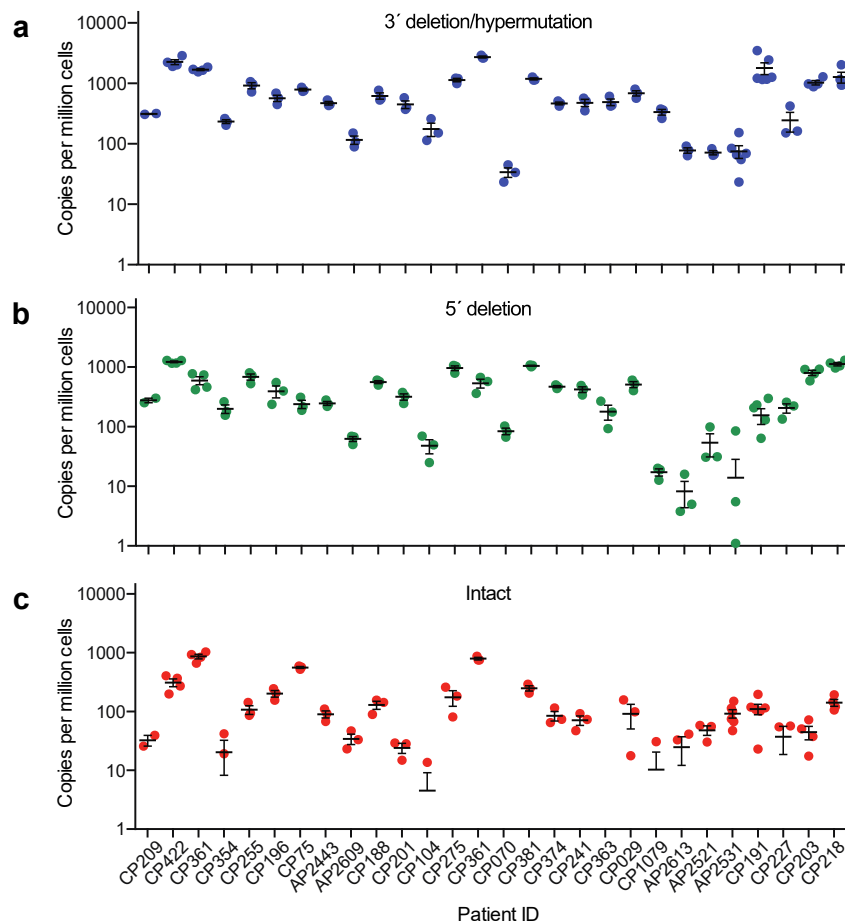


Fig. 9: IPDA reproducibility. Frequencies of cells containing proviruses with 3' deletions and/or hypermutation (A), 5' deletions (B), or no defects (intact) (C) in CD4+ T cells from 28 treated patients. Each data point represents a replicate IPDA determination from a single sample from the indicated patient. The mean and SEM of the replicates are plotted. The variability between patients is much greater than the variation between replicates from a single patient.

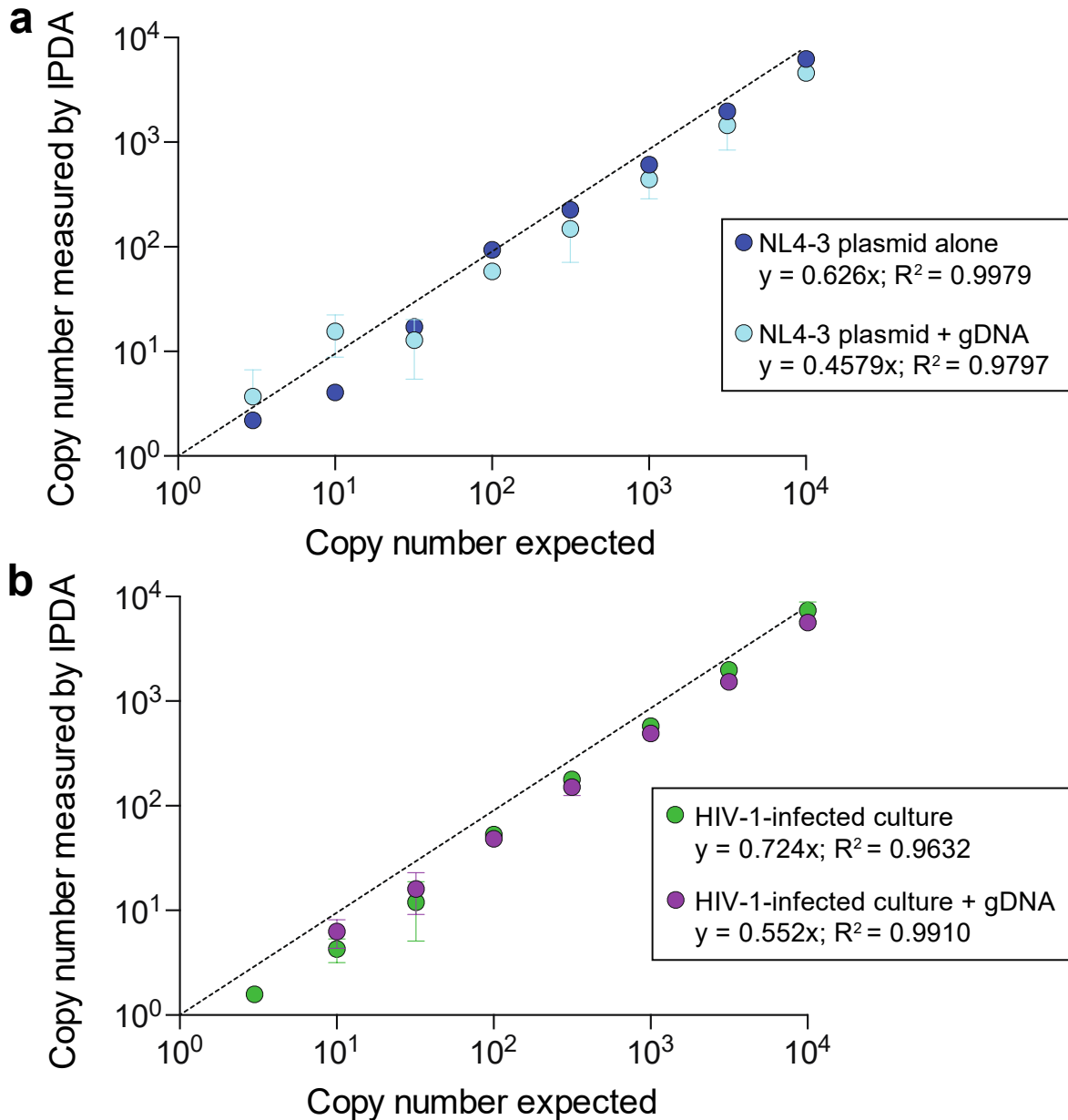


Fig. 10: Linearity of the IPDA.

(A) Standard curve generated using dilutions of the intact proviral reference plasmid NL4-3, with (light blue) or without (dark blue) added genomic DNA (gDNA) from HIV-1-negative PBMCs.

(B) Standard curve generated a characterized an HIV-1 infected cell line with (purple) or without (green) added gDNA. The HIV-1 cell line was generated by infecting Jurkat cells with a single-round GFP virus and sorting for GFP+ cells. The culture was further characterized to verify it contained the correct HIV-1 sequence and approximately one HIV-1 provirus per cell. The mean and standard deviation for each condition are plotted.

HIV latent reservoir change measured by QVOA and IPDA

We next sought to determine if the frequency of intact proviruses measured by IPDA correlated with other reservoir measurements. We found strong correlations between IPDA and QVOA measurements on the same samples ($r=0.48$, $p=0.003$, $n=35$, Fig. 8g). Importantly, we did not expect a precise correlation between IPDA and QVOA. Previous studies have demonstrated that the fraction of intact, replication-competent proviruses induced by a single round of T-cell activation in the standard QVOA is small and more rounds of stimulation could induce additional intact proviruses (Fig. 8h). Using full genome sequences, we compared IPDA with the widely used gag PCR with respect to desired assay characteristics. IPDA detects a larger fraction of the total proviral population (Fig. 8i) and separately enumerates intact proviruses and two classes of defective proviruses. Most importantly, the majority of proviruses classified as intact by IPDA lack any defects detectable by full genome sequencing. In contrast, this value is $<10\%$ for standard gag PCR (Fig. 8i). As a result, the IPDA can detect intervention-induced reductions in intact proviruses that would not be apparent in standard assays (Fig. 8i).

The latent reservoir measured by the QVOA undergoes slow decay ($t_{1/2}=44$ months) (26, 100). To determine whether intact proviruses measured by IPDA show similar decay, we examined longitudinal samples from treated patients taken 2-8 years apart (Fig. 11a). For most patients, intact proviruses declined with a $t_{1/2}$ of ~ 44 months (Fig. 11a,b). Some patients showed even slower decay ($t_{1/2}=100-300$ months), and for 3/14 patients, there was no decay (Fig. 11b,c). Thus the IPDA can measure changes consistent with known reservoir dynamics and possibly define subpopulations with different dynamics. Remarkably, the dynamics of defective proviruses in the same patients showed much greater variability, with increases over time in some patients (Fig. 11a,c), which likely reflects proliferation of cells harboring defective proviruses. While the mean decay slopes were similar, the standard deviations of decay slopes were much greater for defective proviruses, complicating interpretation of assays that are dominated by these defective forms.

Differential dynamics of cells carrying intact and defective proviruses

Increases in infected cell frequency can reflect the proliferation of infected cells (63-68, 70, 101). We asked whether the differential dynamics of cells with intact and defective proviruses could be due to uneven distribution in subsets of memory CD4+ T-cells with different proliferative potential. Intact and defective

proviruses were found in expected ratios in central, transitional, and effector memory subsets (Fig. 11d). We then asked whether intact and defective proviruses imposed different constraints on proliferation of infected cells. We used IPDA to track the fate of individual infected cells from treated patients following in vitro weekly stimulation with anti-CD3/28 (Fig. 11e). Microcultures seeded with ~1 infected cell/well were subjected to 4 rounds of stimulation in the presence of antiretroviral drugs prior to DNA isolation for IPDA, integration site analysis, and full genome sequencing. Analysis of >1700 microcultures showed that positive droplets were detected in only one of three possible quadrants for most positive wells, as expected for cultures initiated with a single infected cell (Fig. 11e). Most (97.6%) proviruses were defective (Fig. 11f). Importantly, the IPDA also counts proviruses in each well allowing direct quantitation of infected cell proliferation. Some cells carrying defective proviruses were capable of enormous clonal expansion (up to 1000 fold) while cells with intact proviruses were rarely detected and showed little proliferative potential (Fig. 11f). These results demonstrate a profound proliferative defect in response to TCR stimulation for cells carrying intact proviruses relative to cells with defective proviruses.

To determine whether proliferative potential was related to the site of integration (64, 65, 101), we analyzed integration sites of expanded clones as previously described (102). This analysis confirmed the clonality of these cultures and that integration in genes with cancer association was not required for proliferation (Fig. 11f, Table 3). Rather we hypothesized that proliferative potential was related to proviral defects. Full genome sequencing confirmed the clonal nature of the proviruses in each well and demonstrated directly that the IPDA correctly identifies the presence and nature of defects in proviruses (Fig. 11g). Of 12 clonally expanded proviruses sequenced, 9 were defective in all HIV-1 ORFs, and none were fully competent for expression of Tat or of Vif, Vpr, Vpu, Env, or Nef. Low or absent expression of these genes would allow stimulated cells to escape viral cytopathic effects that could limit proliferation (84, 85).

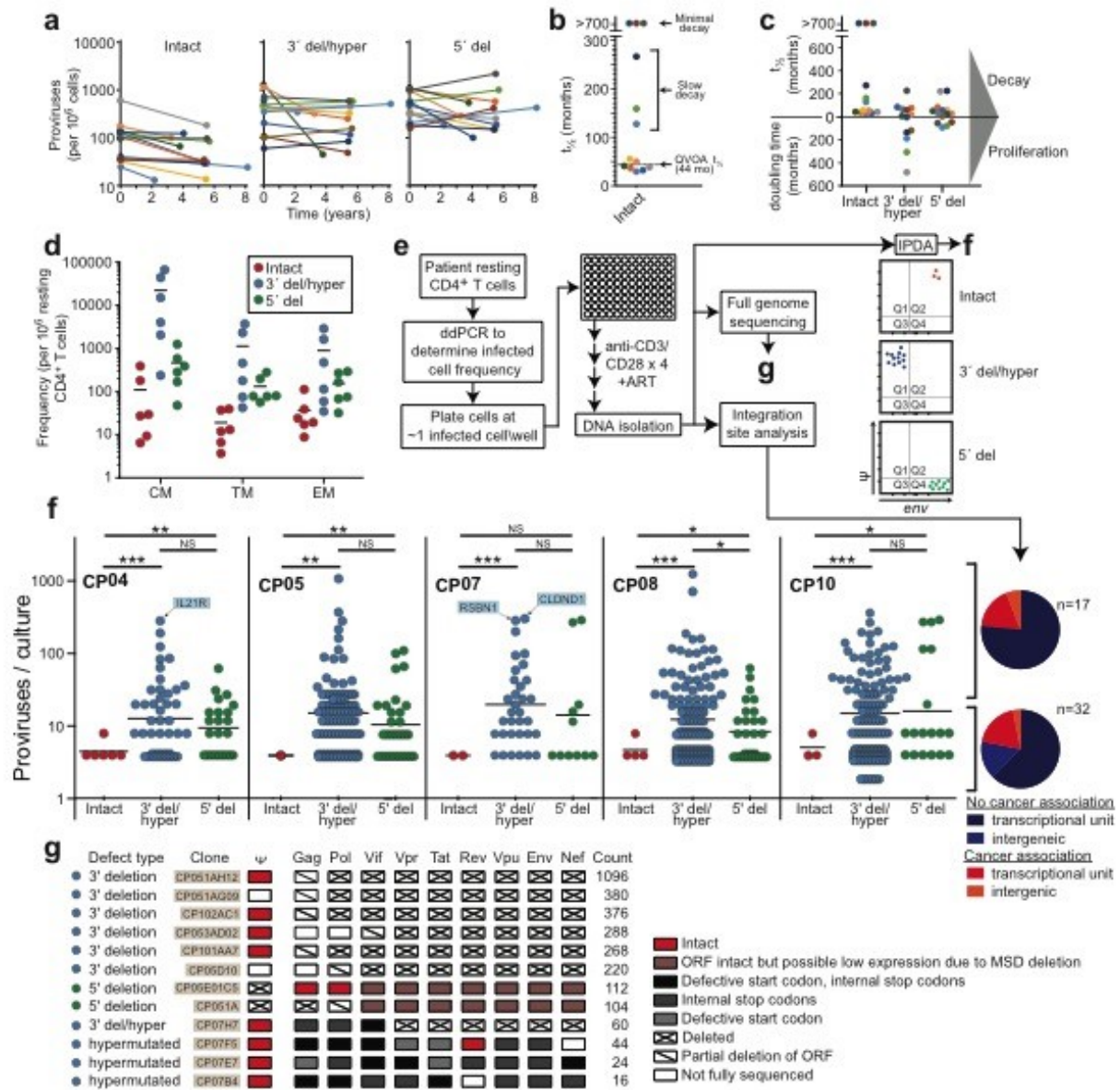


Fig. 11: IPDA reveals differential dynamics of intact and defective proviruses.

(A) Decay of intact proviruses, proviruses with 3' deletion and/or hypermutation (3' del/hyper), and proviruses with 5' deletions (5' del) measured in resting CD4⁺ T cells from patients on long term suppressive ART. Time scale indicates years between sampling.

(B) Half-lives of cells carrying intact proviruses calculated assuming exponential decay from the data in (a). Arrow indicates that t_{1/2} of the latent reservoir determined through QVOA.

(C) Half-lives of populations of cells carrying intact and defective proviruses. For some patients, cells with defective proviruses increased over the time interval shown in (a), and thus a doubling time is displayed.

(D) Distribution of intact and defective proviruses in memory CD4⁺ T-cell subsets.

(E) Experimental system for examining the proliferation of infected cell clones. Resting CD4⁺ T-cells were isolated from patients on ART. The total number of proviruses was measured using a standard gag PCR that detects both intact and defective proviruses (Fig. 6). After correction for gag deleted proviruses, cells were diluted to approximately 1 infected cell per well (2000-4000 total resting CD4⁺ T-cells/well) and subjected 2-4 rounds of stimulation with anti-CD3+anti-CD28 microbeads in the presence of IL-2 and antiretroviral drugs as described in Methods. Over the course of this culture, the cells in each well expanded to an average of 2x10⁶ cells/well. DNA was isolated for IPDA and for integration site analysis and full genome sequencing,

performed as previously described. IPDA analysis generally showed positive droplets in only one of the three possible quadrants, confirming the clonal nature of the cultures and the efficacy of the antiretroviral drugs.

(F) IPDA and integration site analysis of 1731 microcultures from 5 patients. Y-axis indicated number of proviruses in each positive culture. Colors indicate type of provirus detected. Bars indicate geometric mean number of proviruses per culture for each type of proviruses. The statistical significance of differences between numbers of proviruses per positive culture for each type is given at the top of each panel (* = $p < 0.05$, ** = $p < 0.01$, *** = $p < 0.005$). Integrations site analysis was performed on positive cultures as described in Methods. Sites for some of the clones with the highest levels of proliferation are indicated in blue boxes. Pie charts indicate the fractions of integration sites in transcriptional units, intergenic regions, or with cancer associations for cultures with high (> 20 proviruses, top) or low (< 20 proviruses, bottom) proliferation.

(G) Full genome sequencing results for cultures showing proliferation. Sequences were analyzed for defects affecting expression of each HIV-1 gene as described in the legend to Fig. 6b. Count indicates the number of proviruses per culture as detected by IPDA.

Discussion

The failure of cells carrying intact proviruses to expand in response to TCR stimulation provides insights into the mechanisms driving in vivo expansion of cells capable of producing infectious virus and into cure strategies involving T-cell activation. So far, several mechanisms have been proposed to induce proliferation of HIV-infected CD4+ T cells, including antigen stimulation, homeostatic proliferation and proliferation dependent on HIV integration site (64, 65, 70, 101). Our results suggest that antigen stimulation through CD3/CD28 costimulation is likely to induce viral expression in CD4+ T cells carrying replication-competent provirus, leading to cell death. This hypothesis is consistent with our observation that cellular clones carrying replication-competent HIV wax and wane on a time scale of years rather than persisting overtime. Therefore the role of antigen stimulation in HIV persistence requires further investigation. Additionally, we have shown previously that proliferation of HIV-infected cells is common in infected individuals and the extent of proliferation is significant. Therefore the slow decay of the latent reservoir measured by QVOAs must reflect ongoing proliferation balanced by cell death (103). Certain level of T-cell activation may speed up the decay of cells carrying intact proviruses since they showed limited proliferation potential upon TCR stimulation. Mathematical modeling suggests that a 20% reduction in proliferation rate could dramatically decrease the half-life of the latent reservoir. Therefore we should reconsider the possibility of shock and kill strategy and include latency-reversing agents that induce some level of viral

expression in infected cells without causing global T cell activation. Our results show that the small subset of proviruses with the potential to cause viral rebound show different dynamics than the vast excess of defective proviruses captured in standard PCR assays, emphasizing the importance of direct measurement of intact proviruses. Limit of detection and dynamic range are two of the biggest constraints of current assays, especially in the context of interventions studies and large-scale clinical trials involving new cure strategies. As discussed above, PCR-based assays that are used in most current studies are efficient but they could not distinguish intact from defective proviruses that are clinically irrelevant. Assays that allow direct quantification of replication-competent proviruses are time-consuming and give us an underestimate of the reservoir size. The availability of a scalable assay for direct measurement of intact proviruses should accelerate cure research.

Table 1: Characteristics of HIV-1 infected study participants for Chapter 1

| Study ID | Age | Sex | Year of HIV diagnosis | CD4 nadir | Years on ART | ART regimen |
|----------|-----|-----|-----------------------|-----------|--------------|------------------|
| S01 | 55 | F | 1995 | 204 | 10 | RPV/FTC/TAF/DTG |
| S02 | 59 | F | 2004 | 159 | 10 | FTC/TAF |
| S03 | 52 | F | 1999 | 320 | 18 | ABC/DTG/3TC |
| S04 | 55 | M | 1994 | 162 | 10 | EFV/FTC/TAF |
| S05 | 67 | M | 1992 | unknown | 25 | ABC/ETR/3TC/RAL |
| S06 | 54 | F | 1998 | 89 | 10 | DRV/r, FTC, RAL |
| S07 | 57 | F | 1990 | 328 | 8 | DRV, RAL/r, MVC |
| S08 | 51 | M | 1990 | 39 | 15 | DRV/COBI/DTG |
| S09 | 38 | F | 1992 | 275 | 6 | ABC/DTG/3TC |
| S10 | 53 | M | 1997 | 184 | 10 | FTC/RPV/TDF |
| S11 | 63 | M | 2001 | 41 | 16 | FTC/RPV/TAF |
| S12 | 44 | M | 1994 | 105 | 9 | EVG/COBI/FTC/TAF |
| S13 | 61 | M | 1996 | 214 | 21 | DTG, 3TC, DRV/r |
| S14 | 55 | M | 1991 | 8 | 10 | EVG/COBI/FTC/TAF |
| S15 | 69 | M | 1994 | 144 | 14 | DRV, DTG/r |
| S16 | 54 | M | 1998 | 113 | 9 | FTC/RPV/TDF |

Drug abbreviations ABC, abacavir; COBI, cobicistat; DR V, darunavir; DTG, dolutegravir; EFV, efavirenz; EVG, elvitegravir; ETR, etravirine; FTC, emtricitabine; MVC, maraviroc; RAL, raltegravir; RP V, rilpivirine; TAF, tenofovir alafenamide; TDF, tenofovir disoproxil fumarate; 3TC, lamivudine; /r , boosted with ritonavir .

Table 2: Characteristics of HIV-1 infected study participants for Chapter 2

| Parti- -pant ID | Age | Sex | Race ^a | ART Regimen ^b | CD4 count ^c (cells/ μ l) | Plasma HIV-1 RNA ^e (copies/ ml) | Time on ART ^d (mo) | Time on ART with HIV RNA <50 ^e (mo) | CP or EC ^f |
|-----------------------|-----|-----|-------------------|--------------------------|--|--|--|--|-----------------------------|
| AP01 | 44 | M | AA | ABC/3TC/DTG | 687 | <20 | 121 | 115 | CP |
| AP02 | 36 | F | AA | EVG/TAF/FTC/COBI | 840 | <20 | 78 | 77 | CP |
| AP04 | 52 | M | W | EVG/TDF/FTC/COBI | NA | <20 | 79.0 | 70 | CP |
| AP05 | 44 | F | AS | ABC/3TC/DTG | NA | <20 | 41.3 | 40 | CP |
| AP07 | 47 | M | W | FTC/TDF, DTG | NA | <20 | 15.2 | 8 | CP |
| AP08 | 40 | M | W | FTC/TDF, RAL | NA | <20 | 32.1 | 28 | CP |
| AP09 | 33 | M | W | ABC/3TC/DTG | NA | <20 | 24.3 | 20 | CP |
| AP10 | 31 | M | AS | ABC/3TC/DTG | NA | <20 | 14.8 | 13 | CP |
| CP01 | 63 | M | AA | ETR, FTC, RAL | 907 | <20 | 101 | 100 | CP |
| CP02 | 61 | M | AA | ABC/3TC, DRV/r, RAL | 423 | <20 | 46 | 44 | CP |
| CP03 | 76 | M | W | ABC/3TC/ZDV, ATZ/r | 635 | <20 | 192 | 177 | CP |
| CP04 | 49 | F | AA | DRV/r, EFV/FTC/TDF | 890 | <20 | 210 | 55 | CP |
| CP04 | 51 | F | AA | EVG/TAF/FTC/COBI | 582 | <20 | 229 | 74 | CP |
| CP05 | 55 | F | AA | ABC, FTC, ETR, RAL | 441 | <20 | 199 | 104 | CP |
| CP06 | 63 | M | W | ABC, 3TC, RAL, ETR | 997 | <20 | 253 | 50 | CP |
| CP07 | 36 | M | AA | EFV/FTC/TDF | NA | <20 | 61 | 55 | CP |
| CP07 | 40 | M | AA | ABC/3TC/DTG | 976 | <20 | 108 | 102 | CP |
| CP08 | 47 | M | AA | ETR, MVC, RAL | 829 | <20 | 163 | 78 | CP |
| CP09 | 50 | M | AA | 3TC, DRV/r, RAL | 1635 | <20 | 143 | 101 | CP |
| CP10 | 58 | M | AA | ETR, DRV/r, RAL | 570 | <20 | >208 | 120 | CP |
| CP11 | 53 | M | W | ABC/3TC/DTG | 912, 1214 | <20 | 43 | 30 | CP |
| CP12 | 54 | M | AA | 3TC/ZDV, EFV, ATV/r | 586 | <20 | 264 | 135 | CP |
| CP13 | 70 | M | W | EFV/FTC/TDF | 665 | <20 | 224 | 161 | CP |
| CP14 | 56 | M | AA | EFV, DRV/r, RAL | 1011 | <20 | 187 | 179 | CP |
| CP15 | 55 | M | AA | EFV, FTC/TAF | 1550 | <20 | 130 | 112 | CP |
| CP16 | 53 | M | AA | FTC/TAF, RAL | 788 | <20 | 108 | 62 | CP |
| CP17 | 57 | F | AA | ABC/3TC/DTG | 802 | <20 | 107 | 92 | CP |
| CP18 | 49 | F | AA | EVG/TAF/FTC/COBI | 1086 | <20 | 52 | 45 | CP |
| CP19 | 53 | F | AA | None | 535 | 2130 | N/A ^g | N/A ^g | CP |
| CP20 | 49 | F | AA | ABC/3TC/DTG | 623 | <20 | 107 | 98 | CP |
| CP21 | 38 | F | AA | ABC/3TC/DTG | 1098 | <20 | 64 | 60 | CP |
| CP22 | 57 | F | AA | DRV/r, MVC, RAL | 976 | <20 | 92 | 90 | CP |
| CP23 | 56 | M | AA | FTC/TAF, DTG | 670 | <20 | 96 | 31 | CP |

| Partici- -pant ID | Age | Sex | Race ^a | ART Regimen ^b | CD4 count ^c (cells/ μ l) | Plasma HIV-1 RNA ^c (copies/ ml) | Time on ART ^d (mo) | Time on ART with HIV RNA <50 ^e (mo) | CP or EC ^f |
|-------------------------|-----|-----|-------------------|--------------------------|--|--|--|--|-----------------------------|
| CP24 | 58 | F | AA | ETR, DRV/r, RAL | 752, 1146 | <20 | 92 | 38 | CP |
| CP25 | 67 | F | AA | FTC/RPV/ TAF | 482 | <20 | 153 | 142 | CP |
| CP26 | 44 | M | AA | EFV/FTC/TDF | 495 454 | <20 | 97 | 94 | CP |
| CP27 | 63 | M | AA | EFV/FTC/TDF | 502 | <20 | 87 | 73 | CP |
| CP28 | 50 | M | AA | DRV/COBI, DTG | 553 | <20 | 121 | 111 | CP |
| CP29 | 60 | M | AA | EFV, ABC/3TC | 452 | <20 | 189 | 151 | CP |
| CP30 | 64 | M | W | ETR, 3TC, TDF | NA ^h | <20 | NA | 127 | CP |
| CP31 | 64 | M | W | NNRTI regimen | 1750, 1748 | <50, <20 | NA | 72, 170 | CP |
| CP33 | 67 | M | W | NNRTI regimen | 659, 721 | <50, <20 | NA | 45, 114 | CP |
| CP35 | 69 | M | AA | PI regimen | 371, 635 | <50, <20 | NA | 8, 74 | CP |
| CP37 | 74 | M | W | PI regimen | 618, 771 | <50, <50 | NA | 19, 85 | CP |
| CP39 | 71 | M | W | NNRTI+PI regimen | 529, 435 | <50, <20 | NA | 91, 151 | CP |
| CP41 | 74 | M | W | NNRTI regimen | NA, 739 | <50, <50 | NA | 65, 130 | CP |
| CP43 | 61 | M | AA | PI regimen | 760, 484 | <50, <20 | NA | 74, 140 | CP |
| CP45 | 49 | M | AA | PI regimen | 296, 655 | <50, <20 | NA | 105, 171 | CP |
| CP47 | 40 | M | W | NNRTI regimen | 715, 768 | <20, <20 | NA | 47, 108 | CP |
| CP49 | 49 | M | W | NNRTI regimen | 599, 931 | <20, <20 | NA | 58, 117 | CP |
| ES24 | 64 | M | AA | None | 1500 | < 20 | N/A | N/A | EC |
| ES3 | 65 | F | AA | None | 1149 | <20 | N/A | N/A | EC |
| ES31 | 64 | F | AA | None | 744 | <20 | N/A | N/A | EC |
| ES46 | 50 | M | AA | None | 612 | <20 | N/A | N/A | EC |
| ES5 | 65 | F | AA | None | 735 | <20 | N/A | N/A | EC |

^aAA, African American; AS, Asian; W, white.

^bStandard drug abbreviations are used. “/” indicates drugs combined into a single pill. For some cryopreserved samples from MACS cohort participants, regimen details are not available an information on whether the regimen contained a non-nucleoside reverse transcriptast inhibitor (NNRTI) or a protease inhibitor (PI).

^cAt time of sampling.

^dTotal time on ART.

^eTime on ART with plasma HIV-1 RNA <50 copies/ml.

Table 3: Integration site analysis from microcultures.

| Pt ID | U3 loci ^a | U5 loci ^b | Gene ^c | Provirus type ^d | Copy number ^e | Expanded clone ^f | In transcriptional unit ^g | CA association ^h |
|-------|----------------------|----------------------|-------------------|----------------------------|--------------------------|-----------------------------|--------------------------------------|-----------------------------|
| CP04 | chr5-80876827 | chr5+80876823 | MSH3 | 3' del/h | 32 | + | | + |
| CP04 | chr5-80876827 | chr5+80876823 | MSH3 | 5' del | 12 | + | | + |
| CP04 | chr19+34451344 | chr19-34451348 | UBA2 | 5' del | 28 | + | + | |
| CP04 | chr19+34451344 | chr19-34451348 | UBA2 | 3' del/h | 32 | + | + | |
| CP04 | chr1-35495247 | chr1+35495243 | KIAA0319L | 3' del/h | 64 | | + | |
| CP04 | chr7-106102652 | chr7+106102648 | SYPL1 | 5' del | 24 | | + | |
| CP04 | chr19+35190297 | chr19-35190301 | FXYD5 | 3' del/h | 20 | | | + |
| CP07 | chr17-32199245 | chr17-32199249 | RHOT1 | 5' del | 16 | | + | |
| CP07 | chr3-98519105 | chr3-98519101 | CLDND1 | 3' del/h | 308 | | + | |
| CP07 | chr1+113782457 | chr1-113782461 | RSBN1 | 3' del/h | 292 | | + | |
| CP07 | chr17-44145548 | chr17-44145552 | C17orf53 | 3' del/h | 96 | | + | |
| CP07 | chr6+136733815 | chr6+136733811 | MAP3K5 | 3' del/h | 8 | | + | |
| CP07 | chr16+27412884 | chr16-27412888 | LOC105369891 | 3' del/h | 8 | | | |
| CP08 | chr16+67046878 | chr16-67046882 | CBFB | 3' del/h | 16 | | + | + |
| CP08 | chr17+42262488 | chr17-42262492 | STAT5B | 3' del/h | 20 | | + | + |
| CP08 | chr17+42240249 | chr17-42240253 | STAT5B | 3' del/h | 24 | | + | + |
| CP08 | chr2+9594060 | chr2-9594064 | YWHAQ | 3' del/h | 56 | | + | |
| CP08 | chr17+60468915 | chr17-60468919 | APPBP2 | 5' del | 12 | | + | |
| CP08 | chr19-47092528 | chr19+47092524 | ZC3H4 | 3' del/h | 4 | | + | |
| CP08 | chr8+60557609 | chr8-60557613 | RAB2A | 3' del/h | 4 | | + | |
| CP08 | chr2+61079679 | chr2-61079683 | KIAA1841 | 3' del/h | 8 | | + | |
| CP08 | chr7-75478021 | chr7+75478017 | POM121C | 3' del/h | 4 | | + | |
| CP08 | chr17+47475167 | chr17-47475171 | MRPL45P2 | 3' del/h | 4 | | + | |
| CP08 | chr15-78491538 | chr15+78491534 | IREB2 | 3' del/h | 4 | | + | |
| CP08 | chrX+79360929 | chrX-79360933 | ITM2A | 3' del/h | 164 | | + | |
| CP08 | chr1-160517973 | chr1+160517969 | SLAMF6 | 3' del/h | 8 | | + | + |
| CP08 | chr6-13719937 | chr6+13719933 | RANBP9 | 3' del/h | 28 | | | |
| CP08 | chr17+42263312 | chr17-42263316 | STAT5B | 3' del/h | 4 | | + | + |
| CP08 | chr6+90030225 | chr6-90030229 | BACH2 | 3' del/h | 8 | | + | + |
| CP08 | chr16-24750574 | chr16+24750570 | TNRC6A | 3' del/h | 8 | | + | |
| CP08 | chr7+128564161 | chr7-128564165 | METTL2B | 5' del | 12 | | | |
| CP08 | chr2+190667403 | chr2-190667407 | NAB1 | 3' del/h | 28 | | + | |
| CP08 | chr7+72887790 | chr7-72887794 | POM121 | 3' del/h | 4 | | + | |
| CP08 | chr19+57845452 | chr19-57845456 | ZNF587B | 3' del/h | 68 | | + | |
| CP08 | chr17+55289949 | chr17-55289953 | HLF | 5' del | 4 | | + | + |
| CP08 | chr11+123370535 | chr11-123370539 | MIR4493 | 3' del/h | 4 | | | |

| Pt ID | U3 loci ^a | U5 loci ^b | Gene ^c | Provirus type ^d | Copy number ^e | Expanded clone ^f | In transcriptional unit ^g | CA association ^h |
|-------|----------------------|----------------------|-------------------|----------------------------|--------------------------|-----------------------------|--------------------------------------|-----------------------------|
| CP08 | chr7-5692004 | chr7+5692000 | RNF216 | 3' del/h | 8 | | + | + |
| CP08 | chr16+30296748 | chr16-30296752 | SMG1P5 | 3' del/h | 16 | | + | |
| CP08 | chr11-75347724 | chr11+75347720 | ARRB1 | 3' del/h | 28 | | + | |
| CP08 | chr5+176497230 | chr5-176497234 | FAF2 | 3' del/h | 160 | | + | |
| CP08 | chr6-42778282 | chr6+42778278 | GLTSCR1L | 5' del | 12 | | + | |
| CP08 | chr6-26915454 | chr6+26915450 | GUSBP2 | 3' del/h | 4 | | + | |
| CP08 | chr6-135036395 | chr6+135036391 | HBS1L | 3' del/h | 4 | | + | |
| CP08 | chr12-65250700 | chr12+65250696 | LEMD3 | 3' del/h | 8 | | | |
| CP08 | chr3-196305363 | chr3+196305359 | TCTEX1D2 | 3' del/h | 4 | | + | |
| CP08 | chr19+12328836 | chr19-12328840 | ZNF563 | 5' del | 4 | | + | |
| CP08 | chr7-110998623 | chr7+110998619 | IMMP2L | 3' del/h | 4 | | + | |
| CP08 | chr13+74007800 | chr13-74007804 | KLF12 | 3' del/h | 4 | | + | |
| CP08 | chr11-73752097 | chr11+73752093 | RAB6A | 3' del/h | 8 | | + | |
| CP08 | chr9+3295869 | chr9-3295873 | RFX3 | 3' del/h | 24 | | + | |
| CP08 | chr9+132308637 | chr9-132308641 | SETX | 3' del/h | 16 | | + | |
| CP08 | chr11-121540206 | chr11+121540202 | SORL1 | 3' del/h | 4 | | + | + |
| CP08 | chr17-61074679 | chr17+61074675 | BCAS3 | 3' del/h | 1280 | | + | + |
| CP08 | chr19-15290881 | chr19+15290877 | BRD4 | 5' del | 24 | | + | + |
| CP08 | chr11-108718192 | chr11+108718188 | DDX10 | 3' del/h | 4 | | + | + |
| CP08 | chr9-3522329 | chr9+3522325 | RFX3 | 5' del | 16 | | + | |
| CP08 | chr12-56044087 | chr12+56044083 | RPS26 | 5' del | 8 | | + | |
| CP08 | chr16+29557050 | chr16-29557054 | SMG1P2 | 3' del/h | 16 | | + | |
| CP08 | chr6+149336745 | chr6-149336749 | TAB2 | 3' del/h | 4 | | + | |
| CP08 | chr16-2493872 | chr16+2493868 | TBC1D24 | 3' del/h | 4 | | + | |
| CP08 | chr17+62510253 | chr17-62510257 | TLK2 | 5' del | 12 | | + | |
| CP08 | chr17-77986110 | chr17+77986106 | TNRC6C | 3' del/h | 8 | | | |

^aIntegration sites were determined using a previously described 10-12 linker ligation method with HIV-1 primers in the U3 region of the 5' LTR and the U5 region of the 3' LTR. Only sites detected with both U3 and U5 primers are reported. This column gives the U3 site.

^bLocation of integration site detected with U5 primer.

^cName of gene containing the integration site. In cases where the integration site is intergenic, the name of the nearest transcriptional unit is given¹³.

^dNature of provirus detected by IPDA in cells from individual microculture wells. 3' del/h indicated provirus with a 3' deletion and/or hypermutation. 5' del indicated provirus with a 5' deletion. Cells with intact proviruses did not expand sufficiently for integration site analysis.

^eNumber of proviruses present in microculture as determined by IPDA droplet count adjusted for fraction of DNA used in IPDA.

^fIdentical integration site detected in >1 independent microculture from a single donor.

^gIntegration site located within a transcriptional unit.

^hIntegration site within or near a gene which has been associated with some form of cancer in previous studies as defined in reference 13.

Table 4: Primers and probes for IPDA.

| Primer Name | HXB2 coordinates | Fluorophore, quencher | Sequence (5→3') |
|---------------------------|------------------------|-----------------------|--------------------------|
| Ψ F | 692-711 | | CAGGACTCGGCTTGCTGAAG |
| Ψ R | 797-775 ^a | | GCACCCATCTCTCTCCTTCTAGC |
| Ψ Probe | 758-740 ^a | FAM, MGB ^b | TTTTGGCGTACTCACCAGT |
| Env F | 7736-7759 | | AGTGGTGCAGAGAGAAAAAAGAGC |
| Env R | 7851-7832 ^a | | GTCTGGCCTGTACCGTCAGC |
| Env intact probe | 7781-7796 | VIC, MGB | CCTTGGGTTCTTGGGA |
| Env hypermut ^c | 7781-7798 | Unlabeled, MGB | CCTTAGGTTCTTAGGAGC |

^aReverse compliment.

^bMGB, minor groove binder.

^cUnlabeled competitor probe.

References

1. Michael S. Gottlieb, Robert Schroff, Howard M. Schanker, Joel D. Weisman, Peng Thim Fan, Robert A. Wolf, and Andrew Saxon (1981) Pneumocystis carinii Pneumonia and mucosal candidiasis in previously healthy homosexual men — evidence of a new acquired cellular immunodeficiency. *N Engl J Med* 305: 1425-1431.
2. Hutter G, Nowak D, Mossner M, Ganepola S, Mussig A, Allers K (2009) Long-term control of HIV by CCR5 Delta32/Delta32 stem-cell transplantation. *N Engl J Med* 360(7): 692-698.
3. Deborah Persaud, Hannah Gay, Carrie Ziemniak, Ya Hui Chen, Michael Piatak, Tae-Wook Chun, Matthew Strain, Douglas Richman, and Katherine Luzuriaga (2013) Absence of detectable HIV-1 viremia after treatment cessation in an infant. *N Engl J Med* 369: 1828-1835.
4. Gary Maartens, Connie Celum, Sharon R Lewin HIV infection: Epidemiology, pathogenesis, treatment, and prevention. *The Lancet* 384(9939): 258-271.
5. Feng, Y., Broder, C. C., Kennedy, P. E. & Berger, E. A. (1996) HIV-1 entry cofactor: Functional cDNA cloning of a seven-transmembrane, G protein-coupled receptor. *Science* 272: 872-877.
6. The β -chemokine receptors CCR3 and CCR5 facilitate infection by primary HIV-1 isolates. (1996) Choe, H. *Cell* 85: 1135-1148.
7. Klaus Strebel., et al (2013) HIV accessory proteins versus host restriction factors. *Curr Opin Virol* 3(6): 1010-1016.
8. Broder S., et al (2010) Twenty-five years of translational medicine in antiretroviral therapy: Promises to keep. *Sci Transl Med* 2(39)
9. Mitsuya H., et al (1985) 3'-azido-3'-deoxythymidine (BW A509U): An antiviral agent that inhibits the infectivity and cytopathic effect of human T-lymphotropic virus type III/lymphadenopathy-associated virus *in vitro*. *Proc Natl Acad Sci USA* 82: 7091-7100.
10. Fischl MA., et al (1987) The efficacy of azidothymidine (AZT) in the treatment of patients with AIDS and AIDS-related complex. A double-blind, placebo-controlled trial. *N Engl J Med* 317: 185-191.
11. Palella, F. J., et al. (1998) Declining morbidity and mortality among patients with advanced human immunodeficiency virus infection. *N Engl J Med* 338: 853-860.
12. Thompson MA., et al (2012) Antiretroviral treatment of adult HIV infection: 2012 recommendations of the international antiviral society — USA panel. *Jama* 308: 387-402.
13. Palmer S., et al (2008) Low-level viremia persists for at least 7 years in patients on suppressive antiretroviral therapy. *Proc Natl Acad Sci USA* 105: 3879-3884.
14. Dinoso, J. B., et al (2009) Treatment intensification does not reduce residual HIV-1 viremia in patients on highly active antiretroviral therapy. *Proc Natl Acad Sci USA* 106: 9403-9408.

15. Yukl, S. A., et al (2010) Effect of raltegravir-containing intensification on HIV burden and T-cell activation in multiple gut sites of HIV-positive adults on suppressive antiretroviral therapy. *Aids* 24: 2451-2460.
16. Gandhi, R. T. et al. (2010) The effect of raltegravir intensification on low-level residual viremia in HIV-infected patients on antiretroviral therapy: A randomized controlled trial. *PLoS Med* 7: e1000321.
17. Dahl V, et al (2011) Raltegravir treatment intensification does not alter cerebrospinal fluid HIV-1 infection or immunoactivation in subjects on suppressive therapy. *J Infect Dis* 204: 1936-1945.
18. Buzón, M. J. et al. (2010) HIV-1 replication and immune dynamics are affected by raltegravir intensification of HAART-suppressed subjects. *Nature Med* 16: 460-465.
19. Hatano, et al (2013) Increase in 2-long terminal repeat circles and decrease in D-dimer after raltegravir intensification in patients with treated HIV infection: A randomized, placebo-controlled trial. *J Infect Dis* 208: 1436-1442.
20. Molitor JA, Walker WH, Doerre S, Ballard DW, Greene WC. (1990) NF-kappa B: A family of inducible and differentially expressed enhancer-binding proteins in human T cells. *Proc Natl Acad Sci U S A* 87(24): 10028-10032.
21. Perelson AS, et al (1997) Decay characteristics of HIV-1-infected compartments during combination therapy. *Nature* 387: 188-191.
22. Chun, Tae-Wook, et al (1995) In vivo fate of HIV-1-infected T cells: Quantitative analysis of the transition to stable latency. *Nat Med* 1(12): 1284-1290.
23. Chun TW, et al (1997) Presence of an inducible HIV-1 latent reservoir during highly active antiretroviral therapy. *Proc Natl Acad Sci U S A* 94(24): 13193-13197.
24. Finzi D, et al (1997) Identification of a reservoir for HIV-1 in patients on highly active antiretroviral therapy. *Science* 278: 1295-1300.
25. Wong JK, et al (1997) Recovery of replication-competent HIV despite prolonged suppression of plasma viremia. *Science* 278(5341): 1291-1295.
26. Finzi D, et al (1999) Latent infection of CD4+ T cells provides a mechanism for lifelong persistence of HIV-1, even in patients on effective combination therapy. *Nat Med* 5: 512-517.
27. Siliciano JD, et al (2003) Long-term follow-up studies confirm the stability of the latent reservoir for HIV-1 in resting CD4+ T cells. *Nat Med* 9(6): 727-728.
28. Dieffenbach CW., et al (2011) Thirty years of HIV and AIDS: Future challenges and opportunities. *Ann Intern Med* 154(11): 766-771.
29. Eisele E., Siliciano RF. (2012) Redefining the viral reservoirs that prevent HIV-1 eradication. *Immunity* 37(3): 377-388.
30. Deeks S.G., et al International AIDS society global scientific strategy: Towards an HIV cure 2016

31. Archin, N.M., et al (2012) Administration of vorinostat disrupts HIV-1 latency in patients on antiretroviral therapy. *Nature* 487: 482-485.
32. Spivak, A. M. et al. (2014) A pilot study assessing the safety and latency-reversing activity of disulfiram in HIV-1-infected adults on antiretroviral therapy. *Clin Infect Dis* 58: 883-890.
33. Prins, J. M. et al. (1999) Immuno-activation with anti-CD3 and recombinant human IL-2 in HIV-1-infected patients on potent antiretroviral therapy. *Aids* 13: 2405-2410.
34. Wei, D. G. et al. (2014) Histone deacetylase inhibitor romidepsin induces HIV expression in CD4 T cells from patients on suppressive antiretroviral therapy at concentrations achieved by clinical dosing. *PLoS Pathog* 10: e1004071.
35. Archin NM., et al (2012) Administration of vorinostat disrupts HIV-1 latency in patients on antiretroviral therapy. *Nature* 487: 482-485.
36. Xing S, et al (2011) Disulfiram reactivates latent HIV-1 in a BCL-2-transduced primary CD4+ T cell model without inducing global T cell activation. *J Virol* 85: 6060-6064.
37. Doyon G, Zerbato J, Mellors JW, Sluis-Cremer N. (2013) Disulfiram reactivates latent HIV-1 expression through depletion of the phosphatase and tensin homolog. . *Aids* 27: F7-F11.
38. Banerjee C, et al (2012) BET bromodomain inhibition as a novel strategy for reactivation of HIV-1. *J Leukoc Biol* 92: 1147-1154.
39. Boehm D, et al (2013) BET bromodomain-targeting compounds reactivate HIV from latency via a tat-independent mechanism. *Cell Cycle* 12: 452-462.
40. Li Z, Guo J, Wu Y, Zhou Q. (2013) The BET bromodomain inhibitor JQ1 activates HIV latency through antagonizing Brd4 inhibition of tat-transactivation. *Nucleic Acids Res* 41: 277-287.
41. Zhu J, et al (2012) Reactivation of latent HIV-1 by inhibition of BRD4. *Cell Rep* 2: 807-816.
42. Reuse S, et al (2009) Synergistic activation of HIV-1 expression by deacetylase inhibitors and prostratin: Implications for treatment of latent infection. *PLoS ONE* 4: 0006093.
43. DeChristopher BA, et al (2012) Designed, synthetically accessible bryostatins potently induce activation of latent HIV reservoirs in vitro. *Nat Chem* 4: 705-710.
44. Kinter AL, Poli G, Maury W, Folks TM, Fauci AS. (1990) Direct and cytokine-mediated activation of protein kinase C induces human immunodeficiency virus expression in chronically infected promonocytic cells. . *J Virol* 64: 4306-4312.
45. Mehla R, et al (2010) Bryostatins modulates latent HIV-1 infection via PKC and AMPK signaling but inhibits acute infection in a receptor independent manner. *PLoS One* 5: e11160.
46. C. Korin Bullen, Gregory M. Laird, Christine M. Durand, Janet D. Siliciano, and Robert F. Siliciano (2014) Novel *ex vivo* approaches distinguish effective and ineffective single agents for reversing HIV-1 latency *in vivo*. *Nat Med* 20(4): 425-429.

47. Archin NM, et al (2009) Expression of latent HIV induced by the potent HDAC inhibitor suberoylanilide hydroxamic acid. . *AIDS Res Hum Retroviruses* 25: 207-212.
48. Contreras X, et al (2009) Suberoylanilide hydroxamic acid reactivates HIV from latently infected cells. *J Biol Chem* 284: 6782-6789.
49. Blazkova J, et al (2012) Effect of histone deacetylase inhibitors on HIV production in latently infected, resting CD4(+) T cells from infected individuals receiving effective antiretroviral therapy. *J Infect Dis* 206: 765-769.
50. Archin N,M., Sung J,Marsh, Garrido,Carolina, Soriano-Sarabia,Natalia & Margolis D,M. Eradicating HIV-1 infection: Seeking to clear a persistent pathogen
51. Erica N. Borducchi, Crystal Cabral, Kathryn E. Stephenson, Jinyan Liu, Peter Abbink, David Ng'ang'a, Joseph P. Nkolola, Amanda L. Brinkman, Lauren Peter, Benjamin C. Lee, Jessica Jimenez, David Jetton, Jade Mondesir, Shanell Mojta, Abishek Chandrashekar, Katherine Molloy, Galit Alter, Jeff M. Gerold, Alison L. Hill, Mark G. Lewis, Maria G. Pau, Hanneke Schuitemaker, Joseph Hesselgesser, Romas Geleziunas, Jerome H. Kim, Merlin L. Robb, Nelson L. Michael, and Dan H. Barouch1. (2016) Ad26/MVA therapeutic vaccination with TLR7 stimulation in SIV-infected rhesus monkeys. *Nature* 540(7632): 284-287.
52. Borducchi E et al. *PGT121 combined with GS-9620 delays viral rebound in SHIV-infected rhesus monkeys*. . 25th Conference on Retroviruses and Opportunistic Infections (CROI 2018), Boston
53. Liang Shan, et al (2017) Transcriptional reprogramming during effector-toMemory transition renders CD4+ T cells permissive for latent HIV-1 infection. *Immunity* 46: 766-775.
54. Day CL, Kaufmann DE, Kiepiela P, Brown JA, Moodley ES, Reddy S, Mackey EW, Miller JD, Leslie AJ, DePierres C, Mncube Z, Duraiswamy J, Zhu B, Eichbaum Q, Altfeld M, Wherry EJ, Coovadia HM, Goulder PJ, Klenerman P, Ahmed R, Freeman GJ, Walker BD. (2006) PD-1 expression on HIV-specific T cells is associated with T-cell exhaustion and disease progression. *Nature* 443: 350-354.
55. Petrovas C, Casazza JP, Brenchley JM, Price DA, Gostick E, Adams WC, Precopio ML, Schacker T, Roederer M, Douek DC, Koup RA. (2006) PD-1 is a regulator of virus-specific CD8+ T cell survival in HIV infection. *J Exp Med* 203: 2281-2292.
56. Trautmann L, Janbazian L, Chomont N, Said EA, Gimmig S, Bessette B, Boulassel MR, Delwart E, Sepulveda H, Balderas RS, Routy JP, Haddad EK, Sekaly RP. (2006) Upregulation of PD-1 expression on HIV-specific CD8+ T cells leads to reversible immune dysfunction. *Nat Med* 12: 1198-1202.
57. Shan L, et al (2012) Stimulation of HIV-1-specific cytolytic T-lymphocytes facilitates elimination of latent viral reservoir after virus reactivation. *Immunity* 36(3): 491-501.
58. Deng K, Perteau M, Rongvaux A, Wang L, Durand CM, Ghiaur G, Lai J, McHugh HL, Hao H, Zhang H, Margolick JB, Gurer C, Murphy AJ, Valenzuela DM, Yancopoulos GD, Deeks SG, Strowig T, Kumar P, Siliciano JD, Salzberg SL, Flavell RA, Shan L, Siliciano RF. (2015) Broad CTL response is required to clear latent HIV-1 due to dominance of escape mutations. *Nature* 517: 381-385.

59. Shan L, Deng K, Shroff NS, Durand CM, Rabi SA, Yang HC, Zhang H, Margolick JB, Blankson JN, Siliciano RF. (2012) Stimulation of HIV-1-specific cytolytic T lymphocytes facilitates elimination of latent viral reservoir after virus reactivation. *Immunity* 39(1): 491-501.
60. Borrow P, Lewicki H, Wei X, Horwitz MS, Peffer N, Meyers H, Nelson JA, Gairin JE, Hahn BH, Oldstone MB, Shaw GM. (1997) Antiviral pressure exerted by HIV-1-specific cytotoxic T lymphocytes (CTLs) during primary infection demonstrated by rapid selection of CTL escape virus. *Nat Med* 3: 205-211.
61. Carolina Garrido, Maria Abad-Fernandez, Marina Tuyishime, Justin J. Pollara, Guido Ferrari, Natalia Soriano-Sarabia and David M. Margolis (2018) IL-15 stimulated natural killer cells clear HIV-1 infected cells following latency reversal ex vivo. *J Virol* 92(12): e00235-18.
62. Tobin NH, *et al* (2005) Evidence that low-level viremias during effective highly active antiretroviral therapy result from two processes: Expression of archival virus and replication of virus. *J Virol* 79(15): 9625-34.
63. Bailey JR, *et al* (2006) Residual human immunodeficiency virus type 1 viremia in some patients on antiretroviral therapy is dominated by a small number of invariant clones rarely found in circulating CD4+ T cells. *J Virol* 80(13): 6441-6457.
64. Wagner TA, *et al* (2014) HIV latency. proliferation of cells with HIV integrated into cancer genes contributes to persistent infection. *Science* 345(6196): 570-573.
65. Maldarelli F, *et al* (2014) HIV latency. specific HIV integration sites are linked to clonal expansion and persistence of infected cells. *Science* 345(6193): 179-183.
66. Hosmane N,N., *et al* (2017) Proliferation of latently infected CD4+ T cells carrying replication-competent HIV-1: Potential role in latent reservoir dynamics. *Jem* 214(4): 959.
67. Bui J,K., *et al* (2017) Proviruses with identical sequences comprise a large fraction of the replication-competent HIV reservoir. *PLoS Pathog* 13(3): e1006283.
68. Lorenzi JCC, *et al* (2016) Paired quantitative and qualitative assessment of the replication-competent HIV-1 reservoir and comparison with integrated proviral DNA. *Proceedings of the National Academy of Sciences* 113(49): E7908-E7916.
69. Simonetti FR, *et al* (2016) Clonally expanded CD4+ T cells can produce infectious HIV-1 in vivo. *Proceedings of the National Academy of Sciences* 113(7): 1883-1888.
70. Chomont,Nicolas, *et al* (2009) HIV reservoir size and persistence are driven by T cell survival and homeostatic proliferation. *Nat Med* 15: 893-900.
71. Lee SK, Zhou S, Baldoni PL, Spielvogel E, Archin NM, Hudgens MG, Margolis DM, Swanstrom R. (2017) Quantification of the latent HIV-1 reservoir using ultra deep sequencing and primer ID in a viral outgrowth assay. *J Acquir Immune Defic Syndr* 74(2): 221-228.
72. Ho YC, *et al* (2013) Replication-competent noninduced proviruses in the latent reservoir increase barrier to HIV-1 cure. *Cell* 155(3): 540-551.

73. Bruner K,M., *et al* (2016) Defective proviruses rapidly accumulate during acute HIV-1 infection. *Nat Med* 22(9): 1043-9.
74. Rouzioux C, Melard A, Avettand-Fenoel V. (2014) Quantification of total HIV1-DNA in peripheral blood mononuclear cells. *Methods Mol Biol* 1087: 261-270.
75. Strain MC, Lada SM, Luong T, Rought SE, Gianella S, Terry VH, (2013) Highly precise measurement of HIV DNA by droplet digital PCR. *PLoS One* 8(4): e55943.
76. Finzi D, Hermankova M, Pierson T, Carruth LM & et al (1997) Identification of a reservoir for HIV-1 in patients on highly active antiretroviral therapy. *Science* 278(5341): 1295-300.
77. Chun TW, Engel D, Berrey MM, Shea T, Corey L, Fauci AS (1998) Early establishment of a pool of latently infected, resting CD4(+) T cells during primary HIV-1 infection. *Proc Natl Acad Sci U S A* 95(15): 8869-73.
78. Whitney J,B., *et al* (2014) Rapid seeding of the viral reservoir prior to SIV viraemia in rhesus monkeys. *Nature* 512(7512): 74-7.
79. Bosque,Alberto, Famiglietti,Marylinda, Weyrich A,S., Goulston,Claudia & Planelles,Vicente (2011) Homeostatic proliferation fails to efficiently reactivate HIV-1 latently infected central memory CD4+ T cells. *PLoS Pathog* 7(e1002288)
80. Daniel I. S. Rosenbloom, Oliver Elliott, Alison L. Hill, Timothy J. Henrich, Janet M. Siliciano, and Robert F. Siliciano (2015) Designing and interpreting limiting dilution assays: General principles and applications to the latent reservoir for human immunodeficiency virus-1. *Open Forum Infect Dis* 2(4): ofv123.
81. Tamura K, Nei M & Kumar S (2004) Prospects for inferring very large phylogenies by using the neighbor-joining method. *Proceedings of the National Academy of Sciences of the United States of America* 101(30): 11030-11035.
82. Kumar,Sudhir, Stecher,Glen & Tamura,Koichiro (2016) MEGA7: Molecular evolutionary genetics analysis version 7.0 for bigger datasets. *Molecular Biology and Evolution* 33(7): 1870-1874.
83. Laskey S,B., Pohlmeyer C,W., Bruner K,M. & Siliciano R,F. (2016) Evaluating clonal expansion of HIV-infected cells: Optimization of PCR strategies to predict clonality. . *PLoS Pathog* 12: e1005689.
84. Ho D,D., *et al* (1995) Rapid turnover of plasma virions and CD4 lymphocytes in HIV-1 infection. *Nature* 373: 123-126.
85. Wei,Xiping, *et al* (1995) Viral dynamics in human immunodeficiency virus type 1 infection. *Nature* 373: 117-122.
86. Laird G,M., *et al* (2013) Rapid quantification of the latent reservoir for HIV-1 using a viral outgrowth assay. *PLoS Pathog* 9: e1003398.
87. Detels R, et al (2012) The multicenter AIDS cohort study, 1983 to ... *Public Health* 126: 196-198.

88. Imamichi H, et al (2016) Defective HIV-1 proviruses produce novel protein-coding RNA species in HIV-infected patients on combination antiretroviral therapy. *Proc Natl Acad Sci U S A*
89. Rose, P. P., Korber, B. T. (2000) Detecting hypermutations in viral sequences with an emphasis on G --> A hypermutation. *Bioinformatics* 16: 400-401.
90. Lewinski MK, et al (2005) Genome-wide analysis of chromosomal features repressing human immunodeficiency virus transcription. *J Virol* 79: 6610-6619.
91. Berry CC, et al (2012) Estimating abundances of retroviral insertion sites from DNA fragment length data. *Bioinformatics* 28: 755-762.
92. Sherman E, et al (2016) INSPIRED: A pipeline for quantitative analysis of sites of new DNA integration in cellular genomes. *Mol Ther Methods Clin Dev* 4: 39-49.
93. Hiener B, Horsburgh BA, Eden JS, Barton K, Schlub TE, Lee E, von Stockenstrom S, Odevall L, Milush JM, Liegler T, Sinclair E, Hoh R, Boritz EA, Douek D, Fromentin R, Chomont N, Deeks SG, Hecht FM, Palmer S. (2017) Identification of genetically intact HIV-1 proviruses in specific CD4+ T cells from effectively treated participants. *Cell Rep* 21(3): 813-822.
94. Lee GQ, et al (2017) Clonal expansion of genome-intact HIV-1 in functionally polarized Th1 CD4+ T cells. *J Clin Invest* 127: 2689-2696.
95. Halper-Stromberg, Ariel, et al (2014) Broadly neutralizing antibodies and viral inducers decrease rebound from HIV-1 latent reservoirs in humanized mice. *Cell* 158: 989-999.
96. Borducchi EN, et al (2016) Ad26/MVA therapeutic vaccination with TLR7 stimulation in SIVinfected rhesus monkeys. *Nature* 540: 284-287.
97. Sheehy, A. M., Gaddis, N. C., Choi, J. D. & Malim, M. H. (2002) Isolation of a human gene that inhibits HIV-1 infection and is suppressed by the viral vif protein. *Nature* 418: 648-650.
98. Halper-Stromberg A, et al (2014) Broadly neutralizing antibodies and viral inducers decrease rebound from HIV-1 latent reservoirs in humanized mice. *Cell* 158: 989-999.
99. Jordan, A., Bisgrove, D. & Verdin, E. (2003) HIV reproducibly establishes a latent infection after acute infection of T cells in vitro. *Embo J* 22: 1868-1877.
100. Crooks AM, et al (2015) Precise quantitation of the latent HIV-1 reservoir: Implications for eradication strategies. *J Infect Dis*
101. Cohn LB, et al (2015) HIV-1 integration landscape during latent and active infection. *Cell* 160(3): 420-432.
102. Lewinski MK, et al (2005) Genome-wide analysis of chromosomal features repressing human immunodeficiency virus transcription. *J Virol* 79: 6610-6619.
103. Siliciano J,D., et al Long-term follow-up studies confirm the stability of the latent reservoir for HIV-1 in resting CD4+ T cells.

Curriculum Vitae

The Johns Hopkins University School of Medicine
Zheng Wang

(443)691-0825
jessjesszwang@gmail.com
21231

15 S Collington Ave
Baltimore, MD

Educational History:

Johns Hopkins School of Medicine, Baltimore, MD 2013- Present
Ph.D. in Department of Pharmacology and Molecular Science
Rhodes College, Memphis, TN
Bachelor of Science in Chemistry, GPA: Major 3.85, overall 3.56 2009- 2013

RESEARCH EXPERIENCE

Johns Hopkins School of Medicine, Baltimore, MD 2013- Present
Doctorate Training – Infectious Disease/Immunology, Laboratory of Robert F. Siliciano, M.D., Ph.D.

Project I - Led a multidisciplinary research project that:

- Confirmed the role of antigen-driven and cytokine-induced T cell proliferation in HIV persistence
- Modeled proliferation and contraction of HIV-infected CD4⁺ T cells based on TCR sequencing and HIV integration site sequencing data in collaboration with mathematicians/biostatisticians from Harvard University
- Developed a single cell-cloning assay to simultaneously study HIV integration site and HIV genome in collaboration with computational biologists from University of Pennsylvania

Project II - Drug Screening Project

- Screened ChemBridge DIVERSet library for novel HIV latency-reversing agents using FACS flow cytometry and validated positive hits from screening in HIV model cell lines
- Tested the latency reversing effect of farnesyltransferase inhibitors (FTIs) in collaboration with Merck
- Tested the effect of TLR-7 agonist GS-9620 on CD4⁺ T cells in collaboration with Gilead

St.Jude Children's Research Hospital, Memphis, TN 2011-2013
Structural Biology/Proteomics Intern – Structural Biology Department

Hedgehog signaling pathway project

- Prepared pET28 His-Gli3 constructs by cloning for protein expression
- Updated protein sequence database in proteomics core using C programming language

RESEARCH SKILLS

Immunological: primary cell isolation from human tissue specimens, ELISA, T cell functional studies (cytokine secretion, cell proliferation/activation)

status/cytotoxicity/phenotype characterization), multiparametric flow cytometry, cell sorting, virus handling.

Cell Culture: Primary cell cultures, cell line cultures, single cell cloning.

Drug development: drug screening.

Molecular: RNA and DNA isolation, PCR (primer design), qPCR, RT-qPCR, digital droplet PCR, Sanger sequencing and NGS (library preparation), cloning (site-directed mutagenesis).

Programming: Python and C++.

PUBLICATIONS

1. **Wang Z.**, Gurule E.E., Brennan T.P., Gerold J.M., Kwon J.K., Hosmane N.N., Kumar M., Beg S., Capoferri A.A., Ray S.C., Ho Y.C., Hill A.L., Siliciano J.D., Siliciano R.F. Expanded cellular clones carrying replication-competent HIV-1 persist, wax and wane. Proceedings of the National Academy of Science U.S.A.

2. **Wang Z.**, Simonetti F.R., Siliciano R.F., Laird G.M. Measuring replication-competent HIV-1: advances and challenges in defining the latent reservoir. Retrovirology.

3. Bruner K*, **Wang Z.***, Murray A.J., Simonetti F.R., Sengupta S., Kwon K.J., Timmons A., Laskey S.B., Ho Y.C., Clements J.E., Siliciano J.D., Laird G., Siliciano R.F. Differential dynamics of intact and defective HIV-1 proviruses revealed by a novel quantitative approach.

Manuscript under review.

(*co-first author)

PROFESSIONAL PRESENTATIONS

Oral Abstracts and Posters

1. **Wang Z.**, Kumar M.R., Siliciano J.D., Siliciano R.F. Expanded clones harboring replication-competent virus wax and wane overtime. Conferences on Retroviruses and Opportunistic Infections (CROI). Boston, MA, United States. Poster presentation and oral presentation (2018).

2. Gerold J., Bale M.J., **Wang Z.**, Lee G.Q., Lichterfeld M., Siliciano R.F., Kearney M.F., Hill A.L. Quantifying the turnover of latent HIV: Applications to anti-proliferative therapy. Conferences on Retroviruses and Opportunistic Infections (CROI). Boston, MA, United States. Poster presentation (2018).

3. Bruner K., Murray A.J., Ho Y.C., Laird G., **Wang Z.**, Kwon K.J., Beg S., Timmons A., Laskey S.B., Clements J.E., Siliciano J.D., Siliciano R.F. Novel Paradigm for measuring HIV-1 reservoir allows quantification of intact proviruses. Conferences on Retroviruses and Opportunistic Infections (CROI). Boston, MA, United States. Poster presentation and oral presentation (2018).

4. **Wang Z.**, Siliciano R.F., Ho Y.C. TLR7 agonist induces proliferation of HIV-1-infected CD4+ T cells. Keystone symposia conference, HIV Persistence: Pathogenesis and Eradication (X7). California, United States. Poster presentation (2016).

5. **Wang Z.**, Ho Y.C., Siliciano R.F. Proliferation of CD4+ T cells containing replication-competent HIV-1. Conferences on Retroviruses and Opportunistic Infections (CROI). Seattle, WA, United States. Poster presentation and oral presentation (2016).

6. **Wang Z.**, Lambert L., Mittag T., Interaction of Gli3 and SPOP in Hedgehog Pathway. Undergraduate Research and Creative Activity Symposium (URCAS). Memphis, TN, United States. Poster presentation and oral presentation (2012).

AWARDS/HONORS

| | |
|---|------|
| CROI New Investigator Scholarship | 2017 |
| Keystone Symposia Scholarship | 2016 |
| National Institute of Allergy and Infectious Diseases Scholarship | 2015 |
| Gamma Sigma Epsilon Chemistry Honorary Society | 2012 |
| William Spandow Scholarship in Chemistry | 2012 |